SIAM J. APPL. MATH.
Vol. 75, No. 3, pp. 1193–1224

THE TRANSITION TO A POINT CONSTRAINT IN A MIXED BIHARMONIC EIGENVALUE PROBLEM*

A. E. LINDSAY†, M. J. WARD‡, AND T. KOLOKOLNIKOV§

Abstract. The mixed-order eigenvalue problem $-\delta\Delta^2 u + \Delta u + \lambda u = 0$ with $\delta > 0$, modeling small amplitude vibrations of a thin plate, is analyzed in a bounded two-dimensional domain Ω that contains a single small hole of radius ε centered at some $x_0 \in \Omega$. Clamped conditions are imposed on the boundary of Ω and on the boundary of the small hole. In the limit $\varepsilon \to 0$, and for $\delta = \mathcal{O}(1)$, the limiting problem for u must satisfy the additional point constraint $u(x_0) = 0$. To determine how the eigenvalues of the Laplacian in a domain with a small hole are perturbed by adding the small fourth-order term $-\delta\Delta^2 u$, together with an additional boundary condition on $\partial\Omega$ and on the hole boundary, the asymptotic behavior of the eigenvalues of the mixed-order eigenvalue problem are studied in the dual limit $\varepsilon \to 0$ and $\delta \to 0$. Leading-order behaviors of eigenvalues are determined for three ranges of $\delta \ll 1$: $\delta \ll \mathcal{O}(\varepsilon^2)$, $\delta = \mathcal{O}(\varepsilon^2)$, and $\mathcal{O}(\varepsilon^2) \ll \delta \ll 1$. In the first two of these regimes, the limiting behavior depends of the radius of the hole ε, while in the regime $\mathcal{O}(\varepsilon^2) \ll \delta \ll 1$ the eigenvalue is asymptotically independent of ε. Therefore, it is this regime that provides a transition to the point constraint behavior characteristic of the range $\delta = \mathcal{O}(1)$. The asymptotic results for the eigenvalues are validated by full numerical simulations of the PDE.

Key words. bi-Laplacian, singular perturbations, eigenvalue problems

AMS subject classifications. 35G15, 35B25, 74K20

DOI. 10.1137/140979447

1. Introduction.

The determination of eigenfrequencies and eigenmodes characterizing the small amplitude vibration of thin plates is an important problem in mechanics. In the framework of Kirchhoff–Love plate theory (cf. [21]), an eigenmode of vibration, characterizing the out-of-plane deflection w of the plate, is a nontrivial solution of

$$-D\Delta^2 w + T\Delta w + \rho h\omega^2 w = 0\,, \quad x \in \Omega \subset \mathbb{R}^2\,; \qquad w = \partial_n w = 0\,, \quad x \in \partial\Omega\,, \tag{1.1}$$

that occurs for certain discrete values of ω. Here, ρ is the material density and $D = Eh^3/\left[12(1-\mu^2)\right]$ is the flexural rigidity of the plate defined in terms of Young's modulus E, the plate thickness h, and Poisson's ratio μ, while T is the in-plane tension applied at the edges of the plate. To understand the physical significance of each of the terms in (1.1), it is useful to consider it as the Euler–Lagrange equation of the energy functional

$$\mathcal{E}[\phi] \equiv \int_\Omega \left[\frac{1}{2}\rho h\left(\frac{\partial\phi}{\partial t}\right)^2 + \frac{1}{2}D\left(\Delta\phi\right)^2 + \frac{1}{2}T\left|\nabla\phi\right|^2\right] \mathrm{d}x \tag{1.2}$$

after applying the ansatz $\phi(x,t) = w(x)e^{i\omega t}$. The three terms in the integrand of (1.2)

*Received by the editors July 28, 2014; accepted for publication (in revised form) March 19, 2015; published electronically June 11, 2015.
http://www.siam.org/journals/siap/75-3/97944.html
†Department of Applied and Computational Mathematics and Statistics, University of Notre Dame, South Bend, Indiana 46656 (a.lindsay@nd.edu).
‡Department of Mathematics, University of British Columbia, Vancouver, British Columbia, V6T 1Z2, Canada (ward@math.ubc.ca). This author's work was supported by a grant from NSERC (Canada).
§Department of Mathematics and Statistics, Dalhousie University, Halifax, Nova Scotia, B3H 3J5, Canada (kolokol@mathstat.dal.ca). This author's work was supported by a grant from NSERC (Canada).

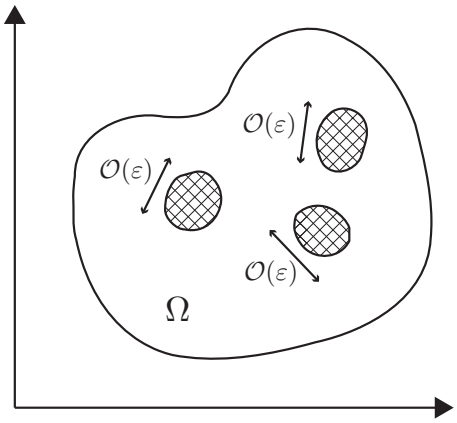

FIG. 1. *Schematic diagram of a perturbed region $\Omega \setminus \Omega_\varepsilon$ consisting of three small holes.*

correspond to the kinetic, bending, and stretching energies of the plate, respectively. In the present work, the density ρ, the thickness h, the flexural rigidity D, and the tension T are taken to be spatially uniform positive constants.

The eigenproblem (1.1), augmented by inserting small clamped holes, can be recast in a more convenient dimensionless form as

$$-\delta\Delta^2 u_\varepsilon + \Delta u_\varepsilon + \lambda_\varepsilon u_\varepsilon = 0\,, \quad x \in \Omega \setminus \Omega_\varepsilon\,; \qquad \int_{\Omega\setminus\Omega_\varepsilon} u_\varepsilon^2 \,\mathrm{d}x = 1\,, \tag{1.3a}$$

$$u_\varepsilon = \partial_n u_\varepsilon = 0\,, \quad x \in \partial\Omega\,; \qquad u_\varepsilon = \partial_n u_\varepsilon = 0\,, \quad x \in \partial\Omega_\varepsilon\,. \tag{1.3b}$$

Here, Ω is a bounded domain in $\mathbb{R}^2$, and Ω_ε is a collection of N small nonoverlapping holes with centers $x_j \in \Omega$ for $j = 0, \ldots, N-1$, for which the jth hole shrinks uniformly to a point $x_j \in \Omega$ as $\varepsilon \to 0$. A schematic representation of the perturbed domain $\Omega \setminus \Omega_\varepsilon$ is shown in Figure 1. In (1.3), the key parameter δ, which reflects the relative importance of the bending and stretching energies, and a new eigenvalue parameter λ_ε are defined by

$$\delta \equiv \frac{D}{T}\,, \qquad \lambda_\varepsilon \equiv \frac{\rho h \omega^2}{T}\,. \tag{1.4}$$

The eigenvalues λ_ε of (1.3) determine the frequencies of vibrations of the perforated thin plate by $\omega = \sqrt{T\lambda_\varepsilon/\rho h}$.

Perforated plate structures are commonly used in many engineering design systems such as heat exchangers in nuclear power systems, sound absorbing screens, or pressure vessels (cf. [7, 4, 16]). In engineering design, drilling a small hole inside a plate is generally the easiest method to alter an undesirable natural frequency of a plate structure without incurring any significant degradation in the structural integrity of the plate (cf. [4, 16]). Effective medium theories, with varying degrees of success, have been used to model the effect of perforations on either the bending of a rectangular plate (cf. [3]) or on the resonant frequencies of a plate (cf. [7, 4]). The development of methodologies to numerically compute resonant frequencies of plates, with and without perforations, are described in [2], [6], and [16].

In this paper, we will use the method of matched asymptotic expansions to analyze (1.3) in the dual limit $\varepsilon \to 0$ and $\delta \to 0$. Before describing our work in detail, we set the context of our study by first briefly summarizing some key previous mathematical results for singularly perturbed biharmonic eigenvalue problems.

From a mathematical viewpoint, the spectrum of the pure biharmonic operator is known to have some rather surprising features owing to the lack of a maximum principle. In a domain with a single small hole Ω_ε of radius ε centered at some $x_0 \in \partial\Omega$, the (pure) biharmonic eigenvalue problem is formulated as

$$\Delta^2 u = \lambda u\,, \quad x \in \Omega \setminus \Omega_\varepsilon\,; \qquad u = \partial_n u = 0\,, \quad x \in \partial\Omega; \tag{1.5a}$$

$$u = \partial_n u = 0\,, \quad x \in \partial\Omega_\varepsilon\,; \qquad \int_{\Omega\setminus\Omega_\varepsilon} u^2\,\mathrm{d}x = 1\,. \tag{1.5b}$$

This system can be obtained formally from (1.3) by setting $N = 1$ and taking the limit $\delta \to +\infty$ while replacing λ by $\delta\lambda$. For the annular domain $0 < \varepsilon \le |x| \le 1$ in two dimensions, it was shown in [8] and [9] that the principal eigenfunction for (1.5) is not radially symmetric when ε is below a critical value. More general results showing that the fundamental mode of vibration for the biharmonic operator is not necessarily of one sign are given in (cf. [22]).

Another key qualitative feature of the spectrum of (1.5), as described in [5], is that the limiting behavior of a simple eigenvalue λ of (1.5) is given by

$$\lambda = \lambda_0 + 4\pi|\nabla u_0(x_0)|^2\nu_b + \mathcal{O}(\nu_b^2), \qquad \nu_b \equiv -\frac{1}{\log\varepsilon}\,, \tag{1.6}$$

where (u_0, λ_0) is an eigenpair of the associated *point constraint problem*

$$\Delta^2 u_0 = \lambda_0 u_0\,, \quad x \in \Omega \setminus \{x_0\}\,; \qquad u_0 = \partial_n u_0 = 0\,, \quad x \in \partial\Omega; \qquad \int_\Omega u_0^2\,\mathrm{d}x = 1\,; \qquad u_0(x_0) = 0\,. \tag{1.7}$$

A remarkable feature of the limiting problem (1.7) is that, due to the additional *point-constraint* requirement $u_0(x_0) = 0$ in (1.7), it is *not* the problem in the absence of a perturbing hole. This result implies that no matter how small ε is made, the vibrational frequencies of the perturbed plate do not approach those of a defect free plate. In [5] and [15], asymptotic expansions for λ were derived for (1.5) to capture higher-order ε-dependent correction terms to (1.6) for both the generic situation where $|\nabla u_0(x_0)| \neq 0$ and for the degenerate case where $|\nabla u_0(x_0)| = 0$. Point constraints also arise in the construction of solutions to nonlinear eigenvalue problems $\Delta^2 u = \lambda f(u)$ in two dimensions [17, 18].

This limiting point constraint behavior for (1.5) as $\varepsilon \to 0$ is qualitatively very different from the well-known results (cf. [19, 12, 14, 23, 24]) for the asymptotic behavior of eigenvalues of the Laplacian in the limit of asymptotically small hole radius $\varepsilon \to 0$, formulated as

$$\Delta u + \lambda u = 0\,, \quad x \in \Omega \setminus \Omega_\varepsilon; \qquad \int_{\Omega\setminus\Omega_\varepsilon} u^2\,\mathrm{d}x = 1; \tag{1.8a}$$

$$u = 0\,, \quad x \in \partial\Omega\,; \qquad u = 0\,, \quad x \in \partial\Omega_\varepsilon\,. \tag{1.8b}$$

For the case of a single hole (N = 1) centered at x_0, it was shown in [23] that the asymptotic behavior of a simple eigenvalue of (1.8) is

$$\lambda \sim \lambda^\star(\nu) + \mathcal{O}\left(\varepsilon\nu\right)\,, \qquad \text{where} \qquad \nu \equiv -1/\log(\varepsilon d)\,, \tag{1.9}$$

and d is the logarithmic capacitance (cf. [20]) associated with the hole. Here, the function $\lambda^\star(\nu)$, which has the effect of summing an infinite logarithmic series in powers

of ν, satisfies a transcendental equation involving the regular part of the Green's function for the Helmholtz operator. As $\nu \to 0$, then $\lambda^\star \to \lambda_0$, where λ_0 is a simple eigenvalue of the following limiting problem in the absence of a hole:

$$\Delta u_0 + \lambda_0 u_0 = 0\,, \quad x \in \Omega\,; \qquad \int_\Omega u_0^2 \,\mathrm{d}x = 1\,; \qquad u_0 = 0\,, \quad x \in \partial\Omega\,. \tag{1.10}$$

With this background, the goal of this paper is to investigate the mixed-order eigenvalue problem (1.3) in the limit $\varepsilon \to 0$ for various ranges of the parameter $\delta > 0$, measuring the relative strength of the fourth-order term. For simplicity, we will only consider the case of a single hole where $N = 1$. For $\delta = \mathcal{O}(1)$, and in the limit $\varepsilon \to 0$ of small hole radius, an eigenvalue of the perturbed problem (1.3) tends to an eigenvalue of the corresponding point constraint problem associated with (1.3) (see (3.1) below). However, the previous analyses of (1.5) and (1.8), as described above, suggest a dichotomy of possible behaviors associated with (1.3) in the dual limit $\varepsilon \to 0$ and $\delta \to 0$. If δ is small enough relative to ε, then the limiting problem as $\varepsilon \to 0$ should be the problem with no hole, whereas if δ is large enough (relative to ε), the limiting problem as $\varepsilon \to 0$ should be one with a point constraint. The goal of this paper is to study the transition between these two cases as $\delta \ll 1$ is varied.

Our analysis on (1.3) reveals that there are three distinguished regimes in the ε, δ plane as $\varepsilon \to 0$ and $\delta \to 0$, where different eigenvalue asymptotics occur. For the regime $\delta \ll \mathcal{O}(\varepsilon^2)$, the leading-order eigenvalue asymptotics for (1.3) is essentially the same as that for the Laplacian, as given in (1.9) (see Principal Result 4.3 below). For the distinguished limit $\delta = \mathcal{O}(\varepsilon^2)$, the leading-order eigenvalue asymptotics as $\varepsilon \to 0$ is again given by (1.9), but where d is replaced by a new quantity $d(\delta_0)$, where $\delta_0 \equiv \delta/\varepsilon^2 = \mathcal{O}(1)$. Here, $d(\delta_0)$ is determined from the far-field behavior of a canonical fourth-order problem defined near the hole (see Principal Result 4.2 below). The third regime is where $\mathcal{O}(\varepsilon^2) \ll \delta \ll \mathcal{O}(1)$. In this regime, we show in Principal Result 4.4 that the leading-order asymptotics of an eigenvalue of (1.3) is given by (1.9), but where εd is replaced by $2\sqrt{\delta}e^{-\gamma_e}$. Since the resulting leading-order eigenvalue asymptotics is independent of the hole radius, it is this regime that provides a transition to the point constraint behavior characteristic of the $\delta = \mathcal{O}(1)$ regime. Finally, in Principal Result 4.5, we improve this leading-order eigenvalue approximation by adding to it a transcendentally small term of order $\mathcal{O}(\sqrt{\delta})$ that results from analyzing the boundary layer near $\partial\Omega$.

The outline of this paper is as follows. In section 2, we study the exactly solvable problem (1.5) in an annular domain in order to clearly motivate the necessity of a point constraint for the limiting solution as $\varepsilon \to 0$. In section 2.2, we formulate and analyze an exactly solvable model biharmonic BVP in an annulus so as to motivate the various scalings in δ and ε that arise in the asymptotic analysis of (1.3). In section 3, we analyze the $\delta \to 0$ limit of the solution to the point constraint problem associated with (1.3) for a single hole. In sections 4.2–4.4, which constitute the main focus of this paper, we will analyze (1.3) for a single hole in the limit $\varepsilon \to 0$ for the three asymptotic ranges of $\delta \ll 1$ given by $\delta = \mathcal{O}(\varepsilon^2)$, $\delta \ll \mathcal{O}(\varepsilon^2)$, and $\mathcal{O}(\varepsilon^2) \ll \delta \ll 1$. For $\delta \ll 1$, the effect of the boundary layer along $\partial\Omega$ on the eigenvalue asymptotics is also examined. In sections 4.4 and 5, we validate our asymptotic theory for the regime $\mathcal{O}(\varepsilon^2) \ll \delta \ll 1$ with full numerical PDE computations of (1.3). Finally, in section 6, we suggest a few open problems that warrant further study.

2. Two exactly solvable model problems. In this section, we present two examples in which the domain is taken to be the annulus $\varepsilon < |x| < 1$ so that $x_0 = (0, 0)$

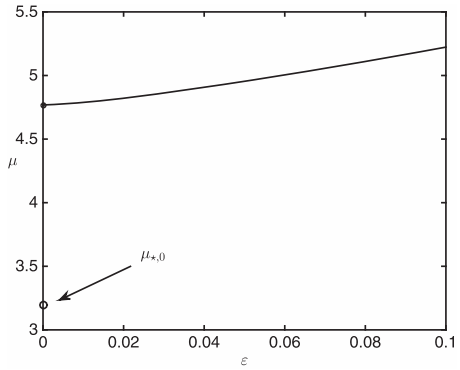

FIG. 2. *The lowest radially symmetric eigenvalue $\mu_{\varepsilon,0}$ versus ε (solid line), as determined from the numerical solution of* (2.2) *on $0 \le \varepsilon \le 0.1$. The limiting value of $\mu_{\varepsilon,0}$ as $\varepsilon \to 0$ is not the lowest eigenvalue $\mu_{\star,0}$ of the unperturbed problem with no hole determined by* (2.1).

and $\Omega_\varepsilon = \{x \,|\, |x| \le \varepsilon\}$. In this setting, closed form solutions can be obtained in terms of Bessel functions. The role of these examples is to develop intuition for the point constraint requirement and the scaling laws associated with the dual limit $\varepsilon \to 0$, $\delta \to 0$. In the first example (cf. section 2.1), we focus on the point constraint problem (1.7) and explicitly determine the jump in the eigenvalue between the hole free and point constraint problem. This formula is verified explicitly in the annulus case for the lowest eigenvalue of the radially symmetric eigenfunctions. The second example (cf. section 2.2) focuses on an exactly solvable mixed problem for which the dual limit $\delta \to 0$, $\varepsilon \to 0$ can be investigated and the transition-to-a-point-constraint regime $\mathcal{O}(\varepsilon^2) \ll \delta \ll 1$ is identified.

2.1. An exactly solvable eigenvalue problem. To obtain exact radially symmetric solutions of (1.5) for the annulus, we factor $\Delta^2 u - \lambda u = (\Delta - \mu^2)(\Delta + \mu^2)u = 0$, where $\mu \equiv \lambda^{1/4}$, so that the separable radially symmetric eigenfunctions are spanned by $\{J_0(\mu r), I_0(\mu r), K_0(\mu r), Y_0(\mu r)\}$, where J_0, I_0, K_0, and Y_0 are Bessel functions. For the $\varepsilon = 0$ problem, with no perturbing hole at the origin, the radially symmetric eigenfunctions $u_\star(r)$ with smooth behavior at the origin are given by

$$u_\star(r) = A\left[J_0(\mu_\star r) - \frac{J_0(\mu_\star)}{I_0(\mu_\star)} I_0(\mu_\star r)\right], \quad \text{where} \quad I_1(\mu_\star)J_0(\mu_\star) + I_0(\mu_\star)J_1(\mu_\star) = 0\,. \tag{2.1}$$

For the annulus, where $\varepsilon > 0$, an exact radially symmetric solution $u_\varepsilon(r)$ is constructed from a linear combination of the set $\{J_0(\mu r), I_0(\mu r), K_0(\mu r), Y_0(\mu r)\}$, such that $u_\varepsilon = \partial_r u_\varepsilon = 0$ on $r = \varepsilon$ and $r = 1$. The eigenvalues of the system, with $\lambda_\varepsilon^{1/4} = \mu_\varepsilon$, are determined by the condition

$$\det \begin{bmatrix} J_0(\mu_\varepsilon) & I_0(\mu_\varepsilon) & K_0(\mu_\varepsilon) & Y_0(\mu_\varepsilon) \\ J_1(\mu_\varepsilon) & -I_1(\mu_\varepsilon) & K_1(\mu_\varepsilon) & Y_1(\mu_\varepsilon) \\ J_0(\varepsilon\mu_\varepsilon) & I_0(\varepsilon\mu_\varepsilon) & K_0(\varepsilon\mu_\varepsilon) & Y_0(\varepsilon\mu_\varepsilon) \\ J_1(\varepsilon\mu_\varepsilon) & -I_1(\varepsilon\mu_\varepsilon) & K_1(\varepsilon\mu_\varepsilon) & Y_1(\varepsilon\mu_\varepsilon) \end{bmatrix} = 0\,. \tag{2.2}$$

In Figure 2, the lowest eigenvalue $\mu_{\varepsilon,0}$, determined from numerical solution of (2.2), is plotted for a range of values of ε. We observe that the limiting behavior of

μ_ε as $\varepsilon \to 0$ is not to an eigenvalue of (2.1) for the problem with no hole. Instead, as shown in [5] and [15], the limiting problem as $\varepsilon \to 0$ requires a point constraint $u_0(0) = 0$, as specified in (1.7). The physical interpretation of this result is that a clamped patch of radius $\mathcal{O}(\varepsilon)$, for any $\varepsilon > 0$, will in general generate an $\mathcal{O}(1)$ jump in the eigenvalue and the vibrational frequencies of the plate.

In the present example of a disk with a puncture at the center, we can construct the radially symmetric eigensolutions of this limiting problem satisfying $u_0(0) = 0$ as

(2.3a)
$$u_0 = A\left[J_0(\mu_0 r) - I_0(\mu_0 r) - \left(\frac{J_0(\mu_0) - I_0(\mu_0)}{\frac{2}{\pi}K_0(\mu_0) + Y_0(\mu_0)}\right)\left(\frac{2}{\pi}K_0(\mu_0 r) + Y_0(\mu_0 r)\right)\right].$$

Here, A is a normalization constant, and μ_0 is a root of the eigenvalue equation

(2.3b)
$$(J_0(\mu_0) - I_0(\mu_0))\left(\frac{2}{\pi}K_1(\mu_0) + Y_1(\mu_0)\right) = (J_1(\mu_0) + I_1(\mu_0))\left(\frac{2}{\pi}K_0(\mu_0) + Y_0(\mu_0)\right).$$

Using the well-known behavior of the Bessel functions for the small argument, we then identify the local behavior as

(2.4)
$$u_0(r) = \alpha_0\, r^2 \log r + \mathcal{O}(r^2), \quad \text{as} \quad r \to 0, \qquad \text{where} \qquad \alpha_0 \equiv \frac{A\mu_0^2\,[J_0(\mu_0) - I_0(\mu_0)]}{2K_0(\mu_0) + \pi Y_0(\mu_0)}.$$

It follows that the limiting eigenfunction u_0 is not smooth at the puncture point but merely differentiable. Moreover, the $r^2 \log r$ singularity structure of (2.4) corresponds to the Green's function for the bi-Laplacian, therefore implying that the clamped patch acts like a Dirac source in the limit $\varepsilon \to 0$.

In terms of this singularity behavior and the constant α_0, we now derive an expression for the difference $\mu_0 - \mu_\star$ between the lowest eigenvalue of the point constraint problem and that of the unperturbed problem. We will derive an expression for this difference in a more general context than an annular domain. We consider the limiting point constraint problem, with $u_0(x_0) = 0$, given by

(2.5a)
$$\Delta^2 u_0 = \lambda_0 u_0, \quad x \in \Omega \setminus \{x_0\}; \qquad u_0 = \partial_n u_0 = 0, \quad x \in \partial\Omega; \qquad \int_\Omega u_0^2\,\mathrm{d}x = 1;$$

(2.5b)
$$u_0(x) \sim \alpha_0 |x - x_0|^2 \log|x - x_0| + \nabla_x R(x; x_0)|_{x=x_0} \cdot (x - x_0) + \mathcal{O}(|x - x_0|^2), \quad \text{as} \quad x \to x_0,$$

and the problem in the absence of a hole, with smooth solution $u_\star$, satisfying

$$\Delta^2 u_\star = \lambda_\star u_\star, \quad x \in \Omega; \qquad u_\star = \partial_n u_\star = 0, \quad x \in \partial\Omega; \qquad \int_\Omega u_\star^2\,\mathrm{d}x = 1. \tag{2.6}$$

The following result gives an expression for the difference between any two eigenvalues of (2.5) and (2.6).

PRINCIPAL RESULT 2.1. *Let (u_0, λ_0) be any simple eigenpair of the limiting problem* (2.5) *with a point constraint $u_0(x_0) = 0$ and let $(u_\star, \lambda_\star)$ be any simple eigenpair of the problem* (2.6) *with no hole. Then for $\langle u_0, u_\star\rangle \neq 0$,*

$$\lambda_0 - \lambda_\star = -\frac{8\pi\,\alpha_0\,u_\star(x_0)}{\langle u_0, u_\star\rangle}, \qquad \textit{where} \qquad \langle u_0, u_\star\rangle \equiv \int_\Omega u_0 u_\star\,\mathrm{d}x. \tag{2.7}$$

Proof. We use Green's second identity over the domain $\Omega\backslash B(x_0,\sigma)$, where $B(x_0,\sigma)$ is a ball of radius $\sigma \ll 1$ centered at x_0. This yields that

$$
\begin{aligned}
(2.8)\qquad (\lambda_0-\lambda_\star)&\int_{\Omega\backslash B(x_0,\sigma)} u_0u_\star \mathrm{d}x\\
&=\int_{\Omega\backslash B(x_0,\sigma)}(u_\star\Delta^2u_0-u_0\Delta^2u_\star)\,\mathrm{d}x\\
&=\int_{\partial B(x_0,\sigma)}(u_\star\partial_n(\Delta u_0)-\Delta u_0\partial_n u_\star-u_0\partial_n(\Delta u_\star)+\Delta u_\star\partial_n u_0)\,\mathrm{d}s\,.
\end{aligned}
$$

Then, with $r=|x-x_0|$ and $\partial_n=-\partial_r$ on $B(x_0,\sigma)$, we use (2.5b) to calculate as $r\to 0$ that

$$
\begin{aligned}
u_0&\sim \alpha_0 r^2\log r + a_c r\cos\theta + a_s r\sin\theta+\cdots\,,\\
u_{0r}&\sim 2\alpha_0 r\log r+\alpha_0 r + a_c\cos\theta+a_s\sin\theta+\cdots\,,\\
\Delta u_0&\sim 4\alpha_0[\log r+1]+\cdots\,,\quad \partial_r\Delta u_0\sim\frac{4\alpha_0}{r}\,,
\end{aligned}
$$

where $(x-x_0)=r(\cos\theta,\sin\theta)$ and $(a_c,a_s)\equiv\nabla_x R(x;x_0)|_{x=x_0}$. Then, since $u_\star$ is smooth as $x\to x_0$, it follows that only the first term in the boundary integral on $\partial B(x_0,\sigma)$ in (2.8) is nonvanishing in the limit $\sigma\to 0$. Therefore,

$$
\begin{aligned}
(\lambda_0-\lambda_\star)\langle u_0,u_\star\rangle &= -\lim_{\sigma\to 0}\int_{\partial B(x_0,\sigma)} u_\star\partial_r(\Delta u_0)\,\mathrm{d}s\\
&=-\lim_{\sigma\to 0} 2\pi\sigma\left[u_\star(x_0)\frac{4\alpha_0}{\sigma}\right]=-8\pi\,\alpha_0\,u_\star(x_0)\,.
\end{aligned}
$$

In the scenario where $\langle u_0,u_\star\rangle\neq 0$, we recover the result (2.7). ∎

To verify this result in the exactly solvable case of the unit disk with the hole centered at the origin, we can without loss of generality set $A=1$ for the normalization constants in (2.1) and (2.3b) and calculate that

$$
(2.9)\qquad u_\star(0)=1-\frac{J_0(\mu_\star)}{I_0(\mu_\star)},\qquad \alpha_0=\frac{\mu_0^2\,[J_0(\mu_0)-I_0(\mu_0)]}{2K_0(\mu_0)+\pi Y_0(\mu_0)}\,.
$$

For the case of the lowest eigenvalue eigenvalues of (2.1) and (2.3b), we evaluate numerically that

$$
\begin{gathered}
\mu_0=4.7683\,,\qquad \mu_\star=3.1962\,,\qquad u_\star(0)=1.0557\,,\\
\alpha_0=618.2445\,,\qquad \langle u_0,u_\star\rangle=-39.758\,.
\end{gathered}
$$

This yields $\lambda_0-\lambda_\star=\mu_0^4-\mu_\star^4\approx 412.6$ from (2.7) and is in agreement with the numerical results from Figure 2.

2.2. An exactly solvable mixed-order BVP. To motivate the different scalings appearing in sections 3–5 below, it is instructive to consider the following radially symmetric model BVP for $u=u(r)$:

$$
(2.10)\quad -\delta\Delta^2u+\Delta u=1\,,\quad \varepsilon<r<1\,;\qquad u(1)=u_r(1)=0\,,\quad u(\varepsilon)=u_r(\varepsilon)=0\,.
$$

Here, $\Delta u \equiv u_{rr} + r^{-1}u_r$ and $\varepsilon \ll 1$. The particular solution for (2.10) is $r^2/4$, while the homogeneous solution is a linear combination of $\{1, \log r, I_0(r/\sqrt{\delta}), K_0(r/\sqrt{\delta})\}$. In this way, the exact solution to (2.10) is readily obtained as

$$u_\varepsilon = \frac{(r^2-1)}{4} + \left[-\frac{c_\varepsilon}{\sqrt{\delta}} I_0'\left(\frac{1}{\sqrt{\delta}}\right) - \frac{1}{2} - \frac{d_\varepsilon}{\sqrt{\delta}} K_0'\left(\frac{1}{\sqrt{\delta}}\right)\right] \log r + c_\varepsilon\left[I_0\left(\frac{r}{\sqrt{\delta}}\right) - I_0\left(\frac{1}{\sqrt{\delta}}\right)\right] + d_\varepsilon\left[K_0\left(\frac{r}{\sqrt{\delta}}\right) - K_0\left(\frac{1}{\sqrt{\delta}}\right)\right], \tag{2.11a}$$

where the constants c_ε and d_ε satisfy the 2×2 linear system

$$c_\varepsilon\left[I_0\left(\frac{\varepsilon}{\sqrt{\delta}}\right) - \frac{\log\varepsilon}{\sqrt{\delta}} I_0'\left(\frac{1}{\sqrt{\delta}}\right) - I_0\left(\frac{1}{\sqrt{\delta}}\right)\right] + d_\varepsilon\left[K_0\left(\frac{\varepsilon}{\sqrt{\delta}}\right) - \frac{\log\varepsilon}{\sqrt{\delta}} K_0'\left(\frac{1}{\sqrt{\delta}}\right) - K_0\left(\frac{1}{\sqrt{\delta}}\right)\right] = \frac{1}{4} - \frac{\varepsilon^2}{4} + \frac{\log\varepsilon}{2}, \tag{2.11b}$$

$$c_\varepsilon\left[I_0'\left(\frac{\varepsilon}{\sqrt{\delta}}\right) - \frac{1}{\varepsilon} I_0'\left(\frac{1}{\sqrt{\delta}}\right) - \sqrt{\delta} I_0\left(\frac{1}{\sqrt{\delta}}\right)\right] + d_\varepsilon\left[K_0'\left(\frac{\varepsilon}{\sqrt{\delta}}\right) - \frac{1}{\varepsilon} K_0'\left(\frac{1}{\sqrt{\delta}}\right) - \sqrt{\delta} K_0\left(\frac{1}{\sqrt{\delta}}\right)\right] = \frac{\sqrt{\delta}}{2\varepsilon} - \frac{\varepsilon\sqrt{\delta}}{2}. \tag{2.11c}$$

We now investigate three different asymptotic limits of (2.11).

We first suppose that $\delta = \mathcal{O}(1)$ and $\varepsilon \to 0$. In (2.11b) and (2.11c), we use the small argument expansions $K_0'(z) \sim -1/z$, $K_0(z) \sim -\log(z/2) - \gamma_e$, and $I_0(z) \sim 1$ as $z \to 0$ to obtain, after some algebra, that (2.11) reduces to

$$u_\varepsilon \sim u_0 \equiv \frac{r^2}{4} + c_0\left[I_0\left(\frac{r}{\sqrt{\delta}}\right) - 1\right] + d_0\left[K_0\left(\frac{r}{\sqrt{\delta}}\right) + \log r - \log\left(2\sqrt{\delta}\right) + \gamma_e\right], \tag{2.12a}$$

where γ_e is Euler's constant. Here, $c_\varepsilon \sim c_0$ and $d_\varepsilon \sim d_0$ as $\varepsilon \to 0$, where c_0 and d_0 satisfy the linear system

$$c_0\left[I_0\left(\frac{1}{\sqrt{\delta}}\right) - 1\right] + d_0\left[K_0\left(\frac{1}{\sqrt{\delta}}\right) - \log\left(2\sqrt{\delta}e^{-\gamma_e}\right)\right] = -\frac{1}{4},$$

$$c_0 I_0'\left(\frac{1}{\sqrt{\delta}}\right) + d_0\left[K_0'\left(\frac{1}{\sqrt{\delta}}\right) + \sqrt{\delta}\right] = -\frac{\sqrt{\delta}}{2}.$$

The key observation is that the limiting solution (2.12a) satisfies $u_0(1) = u_{0r}(1) = 0$ and the point constraint $u_0(0) = 0$. We emphasize that this limiting behavior for (2.11) as $\varepsilon \to 0$ when $\delta = \mathcal{O}(1)$ is not to the smooth unperturbed solution $u_\star$ in the absence of a hole, which is given by

$$u_\star = \frac{1}{4}\left(r^2 - 1\right) - \frac{\sqrt{\delta}}{2I_0'\left(1/\sqrt{\delta}\right)}\left[I_0\left(\frac{r}{\sqrt{\delta}}\right) - I_0\left(\frac{1}{\sqrt{\delta}}\right)\right]. \tag{2.13}$$

The fact that the limiting solution of (2.10) as $\varepsilon \to 0$ with $\delta = \mathcal{O}(1)$ is not the unperturbed solution $u_\star$ is also apparent from a failure of the method of matched

asymptotic expansions. More specifically, if we were to use (2.13) as the leading-order solution in the outer region, then in the inner region, and with local variable $\rho = r/\varepsilon$, the leading-order inner problem for (2.10) would be $\Delta^2 v = 0$ in $\rho \geq 1$, subject to $v = v_\rho = 0$ on $\rho = 1$ together with the matching condition $v \to u_\star(0)$ as $\rho \to \infty$. Since $u_\star(0) \neq 0$ from (2.13), and v must be a linear combination of $\{1, \log\rho, \rho^2, \rho^2\log\rho\}$, it follows that there is no such solution to this inner problem. This, at least formally, suggests that (2.13) cannot be used as the outer solution for (2.10), and instead we must use the solution u_0 in (2.12) satisfying the point constraint $u_0(0) = 0$ as the outer solution.

The second use of the model problem is to investigate the asymptotic behavior of the solution to (2.10), as δ and ε both tend to zero. Two cases are considered: Case I, in which $\delta = \mathcal{O}(\varepsilon^2)$, and Case II, in which $\mathcal{O}(\varepsilon^2) \ll \delta \ll \mathcal{O}(1)$. For Case I, we set $\delta = \delta_0\varepsilon^2$ in (2.11) and let $\varepsilon \to 0$. Upon using the well-known large argument expansions of $K_0(z)$ and $I_0(z)$ as $z \to \infty$, we obtain after some straightforward, but rather lengthy, algebraic manipulations on (2.11) that

$$d_\varepsilon \sim -\frac{\nu\sqrt{\delta_0}}{4K_0'\left(1/\sqrt{\delta_0}\right)}\,, \qquad \nu \equiv -\frac{1}{\log\left(\varepsilon e^{-\chi}\right)}\,, \tag{2.14a}$$

$$\chi \equiv \frac{\sqrt{\delta_0}K_0\left(1/\sqrt{\delta_0}\right)}{K_0'\left(1/\sqrt{\delta_0}\right)}\,; \qquad c_\varepsilon \sim -\frac{\varepsilon\sqrt{\delta_0}}{I_0'\left(1/\varepsilon\sqrt{\delta_0}\right)}\left(\frac{\nu}{4}+\frac{1}{2}\right)$$

and that the outer limit of (2.11a) becomes

$$u_\varepsilon \sim \frac{(r^2-1)}{4} - \frac{\nu}{4}\log r \qquad \text{for} \quad \mathcal{O}(\varepsilon) \ll r \ll 1 - \mathcal{O}(\delta)\,. \tag{2.14b}$$

As a remark, if we include a boundary layer correction term in order to satisfy $u_r = 0$ on $r = 1$, a composite expansion for this modified asymptotic solution is readily obtained as

$$u_\varepsilon \sim \frac{(r^2-1)}{4} - \frac{\nu}{4}\log r + \sqrt{\delta}\left(\frac{1}{2}-\frac{\nu}{4}\right)\left(1 - e^{-\frac{(1-r)}{\sqrt{\delta}}}\right) \qquad \text{for} \quad \mathcal{O}(\varepsilon) \ll r \leq 1\,. \tag{2.14c}$$

The approximation (2.14b) can also be obtained by using the method of matched asymptotic expansions directly on the BVP (2.10), with the analysis being very similar to that given, in a more general context, below in section 4.2.

Finally, we consider Case II, where $\mathcal{O}(\varepsilon^2) \ll \delta \ll \mathcal{O}(1)$. After some algebra, we obtain from (2.11b) and (2.11c) that

$$d_\varepsilon \sim -\frac{\nu_\infty}{4}\,, \qquad \nu_\infty \equiv -\frac{1}{\log\left(2\sqrt{\delta}e^{-\gamma_e}\right)}\,; \qquad c_\varepsilon \sim -\frac{\sqrt{\delta}}{I_0'\left(1/\sqrt{\delta}\right)}\left(\frac{\nu_\infty}{4}-\frac{1}{2}\right) \tag{2.15a}$$

and that the outer limit of (2.11a) is

$$u_\varepsilon \sim \frac{(r^2-1)}{4} - \frac{\nu_\infty}{4}\log r \qquad \text{for} \quad \mathcal{O}(\sqrt{\delta}) \ll r \ll 1 - \mathcal{O}(\delta)\,. \tag{2.15b}$$

The composite expansion satisfying $u_r = 0$ on $r = 1$ for this asymptotic solution is readily obtained to be

$$u_\varepsilon \sim \frac{(r^2-1)}{4} - \frac{\nu_\infty}{4}\log r + \sqrt{\delta}\left(\frac{1}{2}-\frac{\nu_\infty}{4}\right)\left(1 - e^{-\frac{(1-r)}{\sqrt{\delta}}}\right) \qquad \text{for} \quad \mathcal{O}(\sqrt{\delta}) \ll r \leq 1\,. \tag{2.15c}$$

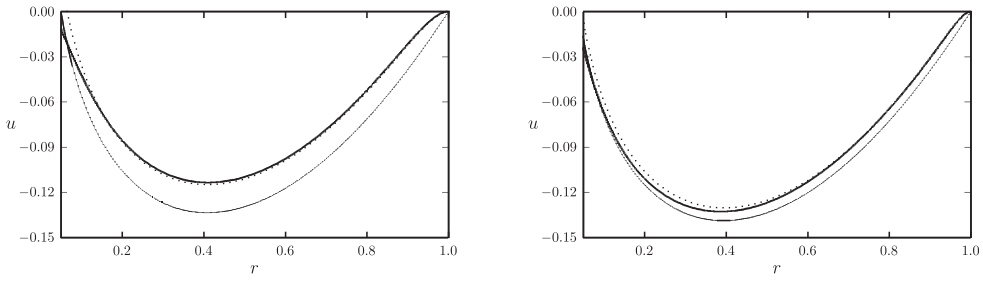

FIG. 3. *Left panel: the exact solution* (2.11) *versus* r *for* $\delta = 0.002$ *and* $\varepsilon = 0.02$ *(heavy solid curve) is compared with the asymptotic solution* (2.15b) *without the boundary layer correction term (solid curve) and with the boundary layer correction term* (2.15c) *(dotted curve). Right panel: similar figure for* $\delta = \varepsilon^2$ *with* $\varepsilon = 0.02$*, so that* $\delta_0 = 1$*. The asymptotic result is given in* (2.14c) *and* (2.14b) *with and without the boundary layer correction term, respectively.*

A key feature of this limiting solution, valid on the range $\mathcal{O}(\varepsilon^2) \ll \delta \ll \mathcal{O}(1)$, is that the outer solution is asymptotically independent of the radius ε of the hole. In this sense, this regime exhibits a *transition to the point constraint behavior* associated with the regime $\delta = \mathcal{O}(1)$. This limiting solution (2.15b) can also be rederived by using the method of matched asymptotic expansions applied to the BVP (2.10), with the analysis being similar to that given below in section 4.4. In Figure 3, we show a favorable comparison between the asymptotic results in (2.14) and (2.15) for Case I and Case II, respectively, and the exact result given in (2.11).

3. The mixed-order eigenvalue problem: Asymptotics of the point constraint problem. As motivated by the analysis in section 2 in the limit $\varepsilon \to 0$, an eigenvalue λ_ε of (1.3) for fixed $\delta = \mathcal{O}(1)$ tends to an eigenvalue λ_0 of the point constraint problem

$$-\delta\Delta^2 u_0 + \Delta u_0 + \lambda_0 u_0 = 0\,, \quad x \in \Omega\backslash\{x_0\}\,; \qquad \int_\Omega u_0^2\,\mathrm{d}x = 1\,, \tag{3.1a}$$

$$u_0 = \partial_n u_0 = 0\,, \quad x \in \partial\Omega\,; \qquad u_0(x_0) = 0\,. \tag{3.1b}$$

The effect of this point constraint is that the smoothness of u_0 is lost in the sense that $\Delta u_0 = \mathcal{O}\left(\log|x - x_0|\right)$ as $x \to x_0$.

To solve (3.1), it is convenient to introduce the Green's function $G_\delta(x; x_0, \lambda_0)$ satisfying

$$\Delta^2 G_\delta - \frac{1}{\delta}\Delta G_\delta - \frac{\lambda_0}{\delta} G_\delta = \delta(x - x_0)\,, \quad x \in \Omega\,; \qquad G_\delta = \partial_n G_\delta = 0\,, \quad x \in \partial\Omega\,. \tag{3.2a}$$

Then, G_δ can be decomposed in terms of a singular part and a C^2 smooth "regular" part $R_\delta(x; x_0, \lambda_0)$ as

$$G_\delta(x; x_0, \lambda_0) = \frac{1}{8\pi}\,|x - x_0|^2 \log|x - x_0| + R_\delta(x; x_0, \lambda_0)\,. \tag{3.2b}$$

As $x \to x_0$, G_δ in (3.2b) has the limiting behavior

$$\begin{aligned} G_\delta(x; x_0, \lambda_0) = \frac{1}{8\pi}\,|x - x_0|^2 \log|x - x_0| + R_\delta(x_0; x_0, \lambda_0) \\ + \nabla_x R_\delta(x; x_0, \lambda_0)|_{x=x_0} + \mathcal{O}(|x - x_0|^2)\,. \end{aligned} \tag{3.3}$$

In terms of G_δ, the solution to (3.1) is simply $u_0 = N_0 G_\delta(x; x_0, \lambda_0)$, where λ_0 is a root of

$$R_\delta(x_0; x_0, \lambda_0) = 0\,, \tag{3.4}$$

and $N_0 = 1/\left(\int_\Omega G_\delta^2\,\mathrm{d}x\right)^{1/2}$. The roots of the point constraint condition (3.4), which is a transcendental equation in λ_0, give the leading-order eigenvalue asymptotics of (1.3) in that $\lambda_\varepsilon \to \lambda_0$, as $\varepsilon \to 0$. We will assume that λ_0 is a root of (3.4) of multiplicity one and that x_0 is such that u_0 satisfies the nondegeneracy condition $\nabla_x R_\delta|_{x=x_0} \neq 0$.

The goal of this section is to derive an approximation to the point constraint condition (3.4) when $\delta \ll 1$. To do so, we will use the method of matched asymptotic expansions to analyze the Green's function of (3.2) as $\delta \to 0$.

In the outer region $\Omega_{\rm out}$, defined as $\Omega_{\rm out} = \{x\,|\,|x-x_0| \gg \mathcal{O}(\sqrt{\delta})$ and $\mathrm{dist}(x, \partial\Omega) \gg \mathcal{O}(\sqrt{\delta})\}$, we expand $G_\delta = \mathcal{G}_0 + o(1)$ to obtain from (3.2a) that

$$\Delta\mathcal{G}_0 + \lambda_0\mathcal{G}_0 = 0\,, \quad x \in \Omega_{\rm out}\,; \qquad \mathcal{G}_0 \to 0\,, \quad \text{as} \quad x \to \partial\Omega\,. \tag{3.5a}$$

This effective zero Dirichlet boundary condition for $\mathcal{G}_0$ as $x \to \partial\Omega$ arises as a leading-order condition for matching $\mathcal{G}_0$ to a boundary-layer solution defined in an $\mathcal{O}(\sqrt{\delta})$ neighborhood of $\partial\Omega$. To construct a solution to (3.2a) that has a singularity at x_0, we first impose that $\mathcal{G}_0$ has a logarithmic singularity as $x \to x_0$, so that

$$\mathcal{G}_0 \sim S\log|x - x_0|\,, \quad \text{as} \quad x \to x_0\,, \tag{3.5b}$$

for some S to be determined. The solution to (3.5) is then simply

$$\mathcal{G}_0 = -2\pi S G_h(x; x_0, \lambda_0)\,, \tag{3.6}$$

where G_h is the Helmholtz Green's function satisfying

$$\Delta G_h + \lambda_0 G_h = -\delta(x - x_0)\,, \quad x \in \Omega\,; \qquad G_h = 0\,, \quad x \in \partial\Omega\,, \tag{3.7a}$$

$$G_h \sim -\frac{1}{2\pi}\log|x - x_0| + R_h(x; x_0, \lambda_0)|_{x=x_0} + \nabla_x R_h(x; x_0, \lambda_0)|_{x=x_0} \cdot (x - x_0) + \cdots\,, \quad \text{as} \quad x \to x_0\,. \tag{3.7b}$$

Here, $R_{h0} \equiv R_h(x; x_0, \lambda_0)|_{x=x_0}$ and $\nabla_x R_{h0} \equiv \nabla_x R_h(x; x_0, \lambda_0)|_{x=x_0}$ are the regular part of the Helmholtz Green's function and its gradient, respectively, which depend on λ_0 and the domain Ω. From (3.6) and (3.7b), it follows that

$$\mathcal{G}_0 \sim S\left[\log|x - x_0| - 2\pi R_{h0} - 2\pi\nabla_x R_{h0}\cdot(x - x_0) + \cdots\right]\,, \quad \text{as} \quad x \to x_0\,. \tag{3.8}$$

This behavior will be used as the matching condition for an inner solution in a neighborhood of x_0. In the inner region, defined in an $\mathcal{O}(\sqrt{\delta})$ neighborhood of x_0, we introduce new variables y and w by

$$y = (x - x_0)/\sqrt{\delta}\,, \qquad w(y) = G_\delta(x_0 + \varepsilon y; x_0, \lambda_0)\,. \tag{3.9}$$

We obtain from (3.2a) that $w \sim w_0 + \cdots$, where w_0 satisfies

$$\Delta_y^2 w_0 - \Delta_y w_0 = 0\,, \quad y \in \mathbb{R}^2\backslash\{0\}\,. \tag{3.10a}$$

In terms of the inner variable, the matching condition as $|y| \to \infty$, as obtained from (3.8), is that

$$w_0 \sim S\log|y| + S\log\sqrt{\delta} - 2\pi S R_{h0} - 2\pi S\sqrt{\delta}\,\nabla_x R_{h0}\cdot y\,, \quad \text{as} \quad |y| \to \infty\,. \tag{3.10b}$$

Moreover, upon substituting the inner scale $y = (x - x_0)/\sqrt{\delta}$ into (3.3), we require that

$$w_0 \sim \frac{\delta}{8\pi}|y|^2 \log|y| + a + b\cdot y + \mathcal{O}(|y|^2)\,, \quad \text{as} \quad y \to 0\,, \tag{3.11}$$

for some scalar a and vector b to be found. We remark that the unknown a represents the limiting asymptotics of $R_\delta(x_0; x_0, \lambda_0)$ as $\delta \to 0$, which we seek to determine.

The solution to (3.10) that is bounded as $y \to 0$ is simply

$$w_0 = S\left[\log|y| + \log\left(\sqrt{\delta}\right) - 2\pi R_{h0} + K_0(|y|)\right] - 2\pi S\sqrt{\delta}\,\nabla_x R_{h0}\cdot y\,, \tag{3.12}$$

where $K_0(|y|)$ is the modified Bessel function of the second kind of order zero. To determine S, we use the well-known refined asymptotics of $K_0(|y|)$ as $|y| \to 0$ from (4.20) below to obtain in terms of Euler's constant $\gamma_e \approx 0.5772$ that

$$w_0 \sim -\frac{S}{4}|y|^2\log|y| + S\left[\log\left(\sqrt{\delta}\right) - 2\pi R_{h0} + \log 2 - \gamma_e\right] - 2\pi S\sqrt{\delta}\,\nabla_x R_{h0}\cdot y\,. \tag{3.13}$$

The final step in the analysis is to choose S so that the $\mathcal{O}(|y|^2\log|y|)$ terms in (3.11) and (3.13) agree, and then identify the constant a in (3.11) from the $\mathcal{O}(1)$ term in (3.13). In this way, we obtain that $S = -\delta/(2\pi)$ and that

$$R_\delta(x_0; x_0, \lambda_0) \sim -\frac{\delta}{2\pi}\left[\log\left(2\sqrt{\delta}\,e^{-\gamma_e}\right) - 2\pi R_{h0}\right]\,, \quad \text{as} \quad \delta \to 0\,. \tag{3.14}$$

Finally, upon substituting (3.14) into the point constraint condition (3.4), it follows for $\delta \to 0$ that λ_0 is a root of

$$R_{h0} = -\frac{1}{2\pi\nu_\infty}\,, \qquad \text{where} \qquad \nu_\infty \equiv -1/\log\left(2\sqrt{\delta}e^{-\gamma_e}\right)\,. \tag{3.15}$$

Here, $R_{h0} \equiv R_h(x_0; x_0, \lambda_0)$ is the regular part of the Helmholtz Green's function as defined by (3.7).

This analysis of the limiting behavior as $\delta \to 0$ of the point constraint condition (3.4) is insufficient for identifying the range of $\delta \ll 1$ and $\varepsilon \ll 1$ for which (3.15) holds as an approximation to an eigenvalue of (1.3). In the more refined analysis of section 4.4, leading to Principal Result 4.4, it is shown that (3.15) yields the leading-order asymptotics for an eigenvalue of (1.3) on the range $\mathcal{O}(\varepsilon^2) \ll \delta \ll \mathcal{O}(1)$ for a hole Ω_ε of arbitrary shape centered at x_0.

4. Asymptotics for $\delta \to 0$ of the mixed-order eigenvalue problem. In this section, we investigate the limiting behavior as $\delta \to 0$ of the mixed-order problem

$$-\delta\Delta^2 u + \Delta u + \lambda u = 0\,, \quad x \in \Omega \setminus \Omega_\varepsilon\,; \qquad \int_{\Omega\setminus\Omega_\varepsilon} u^2\,\mathrm{d}x = 1\,, \tag{4.1a}$$

$$u = \partial_n u = 0\,, \quad x \in \partial\Omega\,; \qquad u = \partial_n u = 0\,, \quad x \in \partial\Omega_\varepsilon\,. \tag{4.1b}$$

Here, Ω_ε is a hole of diameter $\mathcal{O}(\varepsilon)$ that shrinks uniformly to a point $x = x_0 \in \Omega$ as $\varepsilon \to 0$. In our analysis of (4.1) in sections 4.2–4.4, we will consider the limit $\varepsilon \to 0$ for the three asymptotic ranges of $\delta \ll 1$ given by $\delta = \mathcal{O}(\varepsilon^2)$, $\delta \ll \mathcal{O}(\varepsilon^2)$, and $\mathcal{O}(\varepsilon^2) \ll \delta \ll 1$. For each of these regimes, we will determine asymptotic approximations for any $\mathcal{O}(1)$ simple eigenvalues of (4.1). However, first, in order to isolate the effect of the outer boundary $\partial\Omega$, in section 4.1 we begin by calculating the eigenvalues and eigenfunctions of (4.1) for the case $\delta \ll 1$ when there is no hole.

4.1. Boundary layer at $\partial\Omega$. In this subsection, we analyze the perturbation of the eigenvalues λ due to the fourth-order term $-\delta\Delta^2 u$ with $\delta \ll 1$ in the absence of a hole. Assuming, for simplicity, that the boundary $\partial\Omega$ is C^2, this eigenproblem is

(4.2)
$$-\delta\Delta^2 u + \Delta u + \lambda u = 0\,, \quad x \in \Omega\,; \qquad u = \partial_n u = 0\,, \quad x \in \partial\Omega\,; \qquad \int_\Omega u^2\,\mathrm{d}x = 1\,.$$

In the limit $\delta \to 0$, the formal leading-order problem for (4.2) is $\Delta u + \lambda u = 0$. For this reduced problem, both boundary conditions for u cannot be applied on $\partial\Omega$. To understand how the full boundary conditions are enforced, a boundary layer is introduced in the vicinity of $\partial\Omega$. Since $\partial\Omega$ is arbitrary but smooth, it is convenient to employ an orthogonal system (η, s), where $\eta > 0$ measures the perpendicular distance from $x \in \Omega$ to $\partial\Omega$, while on $\partial\Omega$, s measures arc-length. In terms of these coordinates, valid in a neighborhood of $\partial\Omega$, (4.2) becomes

$$\begin{aligned}(4.3)\quad &-\delta\left[\partial_{\eta\eta} - \frac{\kappa}{1-\kappa\eta}\partial_\eta + \frac{1}{1-\kappa\eta}\partial_s\left(\frac{1}{1-\kappa\eta}\partial_s\right)\right]^2 u \\ &\qquad + \left[\partial_{\eta\eta} - \frac{\kappa}{1-\kappa\eta}\partial_\eta + \frac{1}{1-\kappa\eta}\partial_s\left(\frac{1}{1-\kappa\eta}\partial_s\right)\right] u + \lambda u = 0\,.\end{aligned}$$

Here, $\kappa = \kappa(s)$ is the curvature of $\partial\Omega$ with $\kappa = 1$ for the unit disk. Equation (4.3) is valid when $\eta < 1/\left(\max_{\partial\Omega}\kappa\right)$.

In the inner boundary layer region near $\partial\Omega$ of extent $\mathcal{O}(\delta^{1/2})$, we introduce the inner variables and inner expansion

$$(4.4)\qquad \hat\eta = \eta/\delta^{1/2}\,, \qquad u = \delta^{1/2} v\,, \qquad v = v_0 + \delta^{1/2} v_1 + \delta v_2 + \cdots\,.$$

Upon substituting (4.4) into (4.3) and collecting powers of δ, we obtain the following sequence of problems on $\hat\eta \geq 0$:

$$(4.5a)\qquad -v_{0\hat\eta\hat\eta\hat\eta\hat\eta} + v_{0\hat\eta\hat\eta} = 0\,, \qquad v_0 = v_{0\hat\eta} = 0\,, \quad \text{on} \quad \hat\eta = 0\,,$$

$$(4.5b)\qquad -v_{1\hat\eta\hat\eta\hat\eta\hat\eta} + v_{1\hat\eta\hat\eta} = -2\kappa v_{0\hat\eta\hat\eta\hat\eta} + \kappa v_{0\hat\eta}\,, \qquad v_1 = v_{1\hat\eta} = 0\,, \quad \text{on} \quad \hat\eta = 0\,.$$

To asymptotically match the inner solution to an outer solution, as constructed below, we require that the solution to (4.5) has no exponential growth as $\hat\eta \to +\infty$. In this way, the solution to (4.5) is

(4.6)
$$v_0 = -c_0 + c_0\hat\eta + c_0 e^{-\hat\eta}\,; \qquad v_1 = -c_1 + \left(c_1 - \frac{\kappa c_0}{2}\right)\hat\eta + c_1 e^{-\hat\eta} + \frac{\kappa c_0}{2}\hat\eta^2 + \frac{\kappa c_0}{2}\hat\eta e^{-\hat\eta}\,,$$

where $c_0(s)$ and $c_1(s)$ are to be determined. As $\hat\eta \to \infty$, these solutions have the dominant asymptotic behavior

$$v_0 \sim -c_0 + c_0\hat\eta\,, \qquad v_1 \sim -c_1 + \left(c_1 - \frac{\kappa c_0}{2}\right)\hat\eta + \frac{\kappa c_0}{2}\hat\eta^2\,.$$

In terms of the outer variable $\eta = \delta^{1/2}\hat\eta$, the far-field behavior of the two-term inner expansion is

$$(4.7)\qquad u \sim c_0\eta + \frac{\kappa c_0}{2}\eta^2 + \delta^{1/2}\left[-c_0 + \eta\left(c_1 - \frac{\kappa c_0}{2}\right)\right] + \delta\left[-c_1 + \mathcal{O}(\eta)\right] + \cdots\,.$$

In the outer region, defined away from an $\mathcal{O}(\delta^{1/2})$ distance from $\partial\Omega$, we pose the outer expansion

$$(4.8)\qquad u = u_0 + \delta^{1/2} u_1 + \delta u_2 + \cdots\,.$$

In terms of the boundary-fitted orthogonal coordinate system, the local behavior of this outer solution as $\eta \to 0$ is

$$u \sim u_0 + \eta\partial_\eta u_0 + \frac{\eta^2}{2}\partial_{\eta\eta}u_0 + \delta^{1/2}\left[u_1 + \eta u_{1\eta} + \cdots\right] + \delta\left[u_2 + \cdots\right] + \cdots, \tag{4.9}$$

where u_0, u_1, and their derivatives are to be evaluated on $\eta = 0$. Upon comparing (4.9) with the required matching condition (4.7) and noting that the outer normal derivative $\partial_n u$ on $\partial\Omega$ is simply $\partial_n u = -\partial_\eta u$, we obtain

$$u_0 = 0\,, \qquad u_1 = \partial_n u_0\,, \qquad u_2 = \frac{\kappa}{2}\partial_n u_0 + \partial_n u_1\,, \quad x \in \partial\Omega\,. \tag{4.10}$$

Moreover, from this matching condition, c_0 and c_1 in (4.6) are given by

$$c_0 = -\partial_n u_0\,, \qquad c_1 = -\frac{\kappa}{2}\partial_n u_0 - \partial_n u_1\,, \quad x \in \partial\Omega\,. \tag{4.11}$$

Next, we substitute (4.8), together with the eigenvalue expansion $\lambda = \lambda_0 + \delta^{1/2}\lambda_1 + \delta\lambda_2 + \cdots$, into (4.2), and collect powers of δ, to obtain a sequence of outer problems. The effective boundary conditions as $x \to \partial\Omega$ for these outer problems are given by (4.10). In this way, we obtain that

(4.12a)

$$\Delta u_0 + \lambda_0 u_0 = 0\,, \quad x \in \Omega\,; \qquad u_0 = 0\,, \quad x \in \partial\Omega\,; \qquad \int_\Omega u_0^2\,\mathrm{d}x = 1\,,$$

(4.12b)

$$\Delta u_1 + \lambda_0 u_1 = -\lambda_1 u_0\,, \quad x \in \Omega\,; \qquad u_1 = \partial_n u_0\,, \quad x \in \partial\Omega\,; \qquad \int_\Omega u_0 u_1\,\mathrm{d}x = 0\,,$$

(4.12c)

$$\Delta u_2 + \lambda_0 u_2 = (\lambda_0^2 - \lambda_2)u_0 - \lambda_1 u_1\,, \quad x \in \Omega\,;$$
$$u_2 = \partial_n u_1 + \frac{\kappa}{2}\partial_n u_0\,, \quad x \in \partial\Omega\,; \qquad \int_\Omega (2u_0 u_2 + u_1^2)\,\mathrm{d}x = 0\,.$$

We assume that (u_0, λ_0) is a base eigenpair of (4.12a) of multiplicity one. Solvability conditions are then applied to (4.12b) and (4.12c) to fix the values of λ_1 and λ_2, and the solutions u_1 and u_2 are made unique from the integral constraints in (4.12b) and (4.12c). In terms of the unique u_0 and u_1, the functions $c_0(s)$ and $c_1(s)$, as needed in the inner solution (4.6), are calculated from (4.11). Our result is summarized in the following formal statement.

PRINCIPAL RESULT 4.1. *Let (u_0, λ_0) be an eigenpair of* (4.12a) *with multiplicity one and assume that $\partial\Omega$ is smooth. Then, for $\delta \ll 1$, and with $\kappa(s)$ denoting the curvature of $\partial\Omega$, there is an eigenvalue of* (4.2) *with asymptotics*

(4.13)

$$\lambda(\delta) = \lambda_0 + \delta^{1/2}\left[\int_{\partial\Omega}(\partial_n u_0)^2\,\mathrm{d}s\right] + \delta\left[\lambda_0^2 + \int_{\partial\Omega}\partial_n u_0(\partial_n u_1 + \frac{\kappa}{2}\partial_n u_0)\,\mathrm{d}s\right] + \mathcal{O}(\delta^{3/2})\,.$$

We conclude that the biharmonic term and the extra boundary condition $\partial_n u = 0$ on $\partial\Omega$ induce an $\mathcal{O}(\sqrt{\delta})$ correction to the eigenvalue of the Laplacian. In the three subsections below, the various scalings $\delta = \delta(\varepsilon)$ that are investigated as $\varepsilon \to 0$ in (4.1) are all such that eigenvalue correction terms due to the boundary layer are asymptotically smaller than those generated by the hole. However, by including a transcendentally small boundary layer contribution to the eigenvalue approximation, a quantitatively more accurate result is obtained at moderately small values of δ.

4.2. The distinguished limit $\delta = \delta_0\varepsilon^2$. In the limit $\varepsilon \to 0$, in this subsection we study the eigenvalue problem

$$-\delta_0\varepsilon^2\Delta^2 u + \Delta u + \lambda u = 0\,, \quad x \in \Omega\,; \qquad \int_{\Omega\setminus\Omega_\mathcal{E}} u^2\,\mathrm{d}x = 1\,, \tag{4.14a}$$

$$u = \partial_n u = 0\,, \quad x \in \partial\Omega\,; \qquad u = \partial_n u = 0\,, \quad x \in \partial\Omega_\mathcal{E}\,, \tag{4.14b}$$

where $\delta_0 = \mathcal{O}(1)$ is a positive parameter controlling the influence of the bi-Laplacian term in (4.14). Our analysis begins by introducing a canonical local problem defined near the hole $\Omega_\mathcal{E}$. In terms of the local variables

$$y = \varepsilon^{-1}(x - x_0)\,, \qquad v(y) = u(x_0 + \varepsilon y)\,, \tag{4.15}$$

we obtain the following inner problem from (4.14):

$$-\delta_0\Delta_y^2 v + \Delta_y v + \varepsilon^2\lambda v = 0\,, \quad y \in \mathbb{R}^2 \setminus \Omega_0\,; \qquad v = \partial_n v = 0, \quad x \in \partial\Omega_0\,, \tag{4.16}$$

where $\Omega_\mathcal{E} = x_0 + \varepsilon\Omega_0$ and Ω_0 is the magnified domain of the hole. We define the *canonical* solution v_c as the solution to (4.16), upon neglecting the $\mathcal{O}(\varepsilon^2)$ term, that satisfies $v_c \sim \log|y|$ as $|y| \to \infty$. As such, v_c is taken to satisfy

$$-\delta_0\Delta_y^2 v_c + \Delta_y v_c = 0\,, \qquad y \in \mathbb{R}^2 \setminus \Omega_0\,; \qquad v_c = \partial_n v_c = 0\,, \quad y \in \partial\Omega_0\,; \tag{4.17a}$$

$$v_c \sim \log|y| + \chi(\delta_0) + o(1)\,, \quad \text{as} \quad |y| \to \infty\,. \tag{4.17b}$$

Here, the $\mathcal{O}(1)$ constant $\chi(\delta_0)$ in the far-field behavior of v_c depends on both δ_0 and the shape of the hole Ω_0. For an arbitrarily shaped hole Ω_0, $\chi(\delta_0)$ must be calculated numerically.

For the special case where $\Omega_\mathcal{E}$ is the circular disk $|x - x_0| \le \varepsilon$, so that Ω_0 is the unit disk $|y| \le 1$, we can find $\chi(\delta_0)$ analytically. To do so, we note that any radially symmetric solution of $-\delta_0\Delta_y^2 v_c + \Delta_y v_c = 0$ is a linear combination of $\{1, \log\rho, K_0(\rho/\sqrt{\delta_0}), I_0(\rho/\sqrt{\delta_0})\}$. Here, $\rho = |y|$ while $I_0(z)$ and $K_0(z)$ denote modified Bessel functions of the first and second kinds of order zero. To ensure that v_c grows only logarithmically as $\rho \to \infty$, we must eliminate the I_0 component. A simple calculation yields that

$$v_c = \log\rho + a + bK_0\left(\rho/\sqrt{\delta}\right)\,; \qquad a = -\frac{\sqrt{\delta_0}K_0\left(1/\sqrt{\delta_0}\right)}{K_1\left(1/\sqrt{\delta_0}\right)}\,, \qquad b = \frac{\sqrt{\delta_0}}{K_1\left(1/\sqrt{\delta_0}\right)}\,. \tag{4.18}$$

Then, upon comparing (4.18) with (4.17b), and using $K_0(z) \to 0$ as $z \to +\infty$, we readily identify $\chi(\delta_0)$ in (4.17b) as

$$\chi(\delta_0) = -\frac{\sqrt{\delta_0}K_0\left(1/\sqrt{\delta_0}\right)}{K_1\left(1/\sqrt{\delta_0}\right)}\,. \tag{4.19}$$

To determine the asymptotics of $\chi(\delta_0)$ as $\delta_0 \to \infty$, we use the well-known asymptotics for $z \to 0$ given by

$$\begin{aligned} K_0(z) &\sim -\log z + \log 2 - \gamma_e - \frac{1}{4}z^2\log z + \frac{z^2}{4}\left(\log 2 + 1 - \gamma_e\right)\,, \\ K_1(z) &\sim \frac{1}{z} + \frac{z}{4}\left(2\gamma_e - 1\right) + \frac{z}{2}\log\left(\frac{z}{2}\right)\,, \end{aligned} \tag{4.20}$$

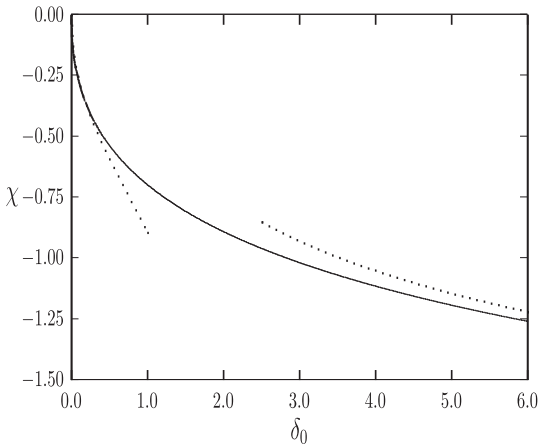

FIG. 4. *Plot of $\chi(\delta_0)$ versus δ_0 for a circular hole of radius ε as computed numerically from* (4.19) *(solid curve). The dotted curves are the approximations in* (4.21) *that are valid for either $\delta_0 \ll 1$ or for $\delta_0 \gg 1$.*

where $\gamma_e \approx 0.5772$ is Euler's constant. In contrast, the asymptotics of $\chi(\delta_0)$ for $\delta_0 \to 0$ relies on the identity $K_0(z)/K_1(z) \sim 1 - 1/(2z) + 51/(128z^2)$ as $z \to \infty$. In this way, we readily calculate that

$$\chi \sim -\log\left(2\sqrt{\delta_0}\right) + \gamma_e - \frac{1}{2\delta_0}\left[\log\left(2\sqrt{\delta_0}\right)\right]^2 + \frac{1}{\delta_0}\left(\gamma_e - \frac{1}{2}\right)\log\left(2\sqrt{\delta_0}\right) - \frac{\left(1 - 2\gamma_e + 2\gamma_e^2\right)}{4\delta_0}, \quad \text{as} \quad \delta_0 \to \infty, \tag{4.21a}$$

$$\chi \sim -\sqrt{\delta_0} + \frac{\delta_0}{2} - \frac{51}{128}\delta_0^{3/2} + \mathcal{O}(\delta_0^2), \quad \text{as} \quad \delta_0 \to 0. \tag{4.21b}$$

In Figure 4, we plot $\chi(\delta_0)$, as computed from (4.19), and compare it with the limiting asymptotic behavior in (4.21).

Finally, it is convenient to introduce the constant $d = d(\delta_0) \equiv e^{-\chi(\delta_0)}$ defined so that

$$v_c \sim \log|y| - \log d + o(1), \quad \text{as} \quad |y| \to \infty; \qquad d \equiv e^{-\chi(\delta_0)}. \tag{4.22}$$

When Ω_ε is the disk of radius ε, d can be calculated from $\chi(\delta_0)$ in (4.19). From (4.21), it has the leading-order behavior

$$d \sim 2\sqrt{\delta_0}\, e^{-\gamma_e}, \quad \text{as} \quad \delta_0 \to \infty; \qquad d \sim 1 + \sqrt{\delta_0} + \mathcal{O}(\delta_0^{3/2}), \quad \text{as} \quad \delta_0 \to 0. \tag{4.23}$$

Next, we construct an infinite asymptotic series in powers of $\nu \equiv -1/\log(\varepsilon d)$ for a simple eigenvalue of (4.1). In terms of the canonical inner solution v_c and unknown constants c_j, we expand the inner solution for (4.16) as

$$v \sim \nu \sum_{j=0}^{\infty} \nu^j c_j v_c, \qquad \nu \equiv -1/\log(\varepsilon d), \qquad d \equiv e^{-\chi(\delta_0)}. \tag{4.24}$$

To determine the far-field behavior of (4.24), we use (4.22) in (4.24) and write the resulting expression in terms of the outer variable. This yields the following matching

condition for the outer solution of (4.1):

$$u \sim c_0 + \sum_{j=1}^{\infty} \nu^j \left[c_{j-1} \log|x - x_0| + c_j \right], \qquad \text{as} \quad x \to x_0 \,. \tag{4.25}$$

In the outer region, where $|x - x_0| \gg \mathcal{O}(\varepsilon)$ and $\operatorname{dist}(x, \partial\Omega) \gg \mathcal{O}(\delta^{1/2}) = \mathcal{O}(\varepsilon)$, we expand the eigenvalue λ and the outer eigenfunction u as

$$u \sim u_0 + \sum_{j=1}^{\infty} \nu^j u_j + \cdots, \qquad \lambda \sim \lambda_0 + \sum_{j=1}^{\infty} \nu^j \lambda_j + \cdots \,. \tag{4.26}$$

Here, $u_0(x)$ and λ_0 is assumed to be any simple eigenpair of the unperturbed problem (4.12a) for which $u_0(x_0) \neq 0$. The leading-order matching condition from (4.25) is that $c_0 = u_0(x_0)$. Since $\nu^j \gg \mathcal{O}(\varepsilon)$ for any $j \geq 0$, the correction to λ_0 induced by the boundary layer near $\partial\Omega$ is asymptotically smaller than any term in the infinite series (4.26). As such, in our analysis of the outer region, we can neglect both the boundary layer near $\partial\Omega$ and the term $-\delta\varepsilon^2\Delta^2$ in (4.1), while imposing $u \to 0$ as $x \to \partial\Omega$. Thus, upon substituting (4.26) into (4.1) and the matching condition (4.25), we obtain upon equating powers of ν that u_j for $j \geq 1$ satisfies

$$\Delta u_j + \lambda_0 u_j = -\lambda_j u_0 - (1 - \delta_{1j}) \sum_{i=1}^{j-1} \lambda_i u_{j-i} u_0 \,, \quad x \in \Omega \backslash \{x_0\} \,; \tag{4.27a}$$

$$u_j = 0 \,, \qquad x \in \partial\Omega \,,$$

$$u_j \sim c_{j-1} \log|x - x_0| + c_j \,, \qquad \text{as} \quad x \to x_0 \,, \tag{4.27b}$$

$$\int_\Omega u_0 u_j \, \mathrm{d}x = -\frac{1}{2}(1 - \delta_{1j}) \sum_{i=1}^{j-1} \int_\Omega u_i u_{j-i} \, \mathrm{d}x \,, \tag{4.27c}$$

where $c_0 = u_0(x_0) \neq 0$ and δ_{1j} is the usual Kronecker symbol.

The coefficients c_j for $j \geq 1$ and the eigenvalue corrections λ_j for $j \geq 1$ are determined recursively from (4.27). Suppose that c_{j-1} and u_i for $0 \leq i \leq j-1$ are known. Then, the solvability condition for (4.27) yields that

$$\lambda_j = 2\pi c_{j-1} u_0(x_0) - (1 - \delta_{1j}) \sum_{i=1}^{j-1} \lambda_i \int_\Omega u_{j-i} u_0 \, \mathrm{d}x \quad \text{for} \quad j \geq 1 \,. \tag{4.28}$$

With λ_j now determined, we can solve (4.27a) with $u_j \sim c_{j-1} \log|x - x_0|$ as $x \to x_0$ to obtain u_j to within an additive multiple of u_0. This multiple is then determined uniquely by the normalization condition (4.27c). Finally, with u_j now uniquely determined, we calculate the constant c_j from the limiting behavior $c_j = \lim_{x \to x_0}(u_j - c_{j-1} \log|x - x_0|)$. This process is repeated recursively in j. It is initialized with $c_0 = u_0(x_0)$, where (u_0, λ_0) is an eigenpair of (4.12a).

We illustrate this procedure by deriving a three-term expansion for λ. For $j = 1$, (4.28) yields that $\lambda_1 = 2\pi[u_0(x_0)]^2$. To identify u_1 from (4.27), it is convenient to introduce the uniquely defined $G_m(x; x_0)$ by

$$\Delta G_m + \lambda_0 G_m = u_0(x_0) u_0(x) - \delta(x - x_0) \,, \quad x \in \Omega \,; \qquad G_m = 0 \,, \quad x \in \partial\Omega \,, \tag{4.29a}$$

$$G_m(x; x_0) \sim -\frac{1}{2\pi} \log|x - x_0| + R_m(x_0) + o(1) \,, \tag{4.29b}$$

$$\text{as} \quad x \to x_0 \,; \qquad \int_\Omega G_m u_0 \, \mathrm{d}x = 0 \,,$$

where $R_m(x_0)$ is the regular part of the modified Green's function G_m. The solution to (4.27) with $j = 1$ is simply

$$u_1 = -2\pi u_0(x_0) G_m(x; x_0)\,. \tag{4.30}$$

Next, expanding u_1 as $x \to x_0$ and comparing with (4.27b) for $j = 1$, we get $c_1 = -2\pi u_0(x_0) R_m(x_0)$. Finally, since $\int_\Omega u_0 u_1 \,\mathrm{d}x = 0$, (4.28) for $j = 2$ yields that $\lambda_2 = -4\pi^2 \left[u_0(x_0)\right]^2 R_m(x_0)$. We summarize the result as follows:

PRINCIPAL RESULT 4.1. *Let (u_0, λ_0) be an simple eigenpair of* (4.12a) *with $u_0(x_0) \neq 0$. Then, for $\delta = \varepsilon^2 \delta_0$ with $\delta_0 = \mathcal{O}(1)$,* (4.14) *has an eigenvalue with three-term asymptotics*

$$\begin{aligned} &\lambda \sim \lambda_0 + 2\pi \left[u_0(x_0)\right]^2 \nu - 4\pi^2 \left[u_0(x_0)\right]^2 R_m(x_0)\nu^2 + \mathcal{O}(\nu^3)\,; \\ &\nu \equiv -1/\log(\varepsilon d)\,, \quad d = e^{-\chi(\delta_0)}\,, \end{aligned} \tag{4.31}$$

where $\chi(\delta_0)$ is defined in (4.17b) *in terms of the far-field behavior of the canonical inner solution v_c. For a circular hole of radius ε, $\chi(\delta_0)$ is given in* (4.19). *Here, $R_m(x_0)$ is the regular part of the modified Green's function in* (4.29).

We conclude this section by deriving a transcendental equation for λ that has the effect of summing the infinite logarithmic series in (4.26). Since the analysis is similar to that in [23], we only briefly outline it here.

In the inner region, the solution to (4.16) is given asympotically in terms of some unknown function $\mathcal{C}(\nu)$ as

$$v \sim \mathcal{C}(\nu)\nu v_c\,. \tag{4.32}$$

Upon using $v_c \sim \log|y| - \log d + o(1)$ as $|y| \to \infty$ in (4.32), we derive the matching condition for the outer solution:

$$u \sim \mathcal{C}\nu \log|x - x_0| + \mathcal{C}\,, \quad \text{as} \quad x \to x_0\,. \tag{4.33}$$

In the outer region, instead of expanding u and λ term-by-term in powers of ν as in (4.26), we expand $u = u^\star(x;\nu) + \text{t.s.t.}$ and $\lambda = \lambda^\star(\nu) + \text{t.s.t.}$, where t.s.t indicates terms that are transcendentally small in comparison with ν. In addition, $u^\star$ is to satisfy the matching condition (4.33). In this way, we find that $u^\star$ and $\lambda^\star$ satisfy

$$\Delta u^\star + \lambda^\star u^\star = 0\,, \qquad x \in \Omega\backslash\{x_0\}\,; \quad u^\star = 0\,, \quad x \in \partial\Omega\,; \qquad \int_\Omega \left[u^\star\right]^2 \,\mathrm{d}x = 1\,. \tag{4.34a}$$

$$u^\star \sim \mathcal{C}\nu \log|x - x_0| + \mathcal{C}\,, \qquad \text{as} \quad x \to x_0\,. \tag{4.34b}$$

The singularity structure (4.34b) specifies both the regular and singular part of the singularity. As such, it provides a constraint to determine $\lambda^\star$. The solution to (4.34) is

$$u^\star = -2\pi \mathcal{C}(\nu) G_h(x; x_0, \lambda^\star)\,, \tag{4.35}$$

where $\mathcal{C}$ is found from the condition $\int_\Omega \left[u^\star\right]^2 \mathrm{d}x = 1$. Here, G_h is the Helmholtz Green's function satisfying

$$\Delta G_h + \lambda^\star G_h = -\delta(x - x_0)\,, \quad x \in \Omega\,; \qquad G_h = 0\,, \quad x \in \partial\Omega\,, \tag{4.36a}$$

$$G_h \sim -\frac{1}{2\pi}\log|x - x_0| + R_h(x_0; \lambda^\star) + o(1)\,, \quad \text{as} \quad x \to x_0\,, \tag{4.36b}$$

where $R_h(x_0;\lambda^\star)$ is the regular part of G_h. Then, by expanding $u^\star$ in (4.35) as $x \to x_0$ and comparing the resulting expression with (4.34b), we get $-2\pi\nu R_h\mathcal{C} = \mathcal{C}$, which is an equation for $\lambda^\star$. We summarize the result as follows.

PRINCIPAL RESULT 4.2. *For $\delta = \varepsilon^2\delta_0$ with $\delta_0 = \mathcal{O}(1)$, there is an eigenvalue λ of* (4.14) *with $\lambda \sim \lambda^\star(\nu) + t.s.t$, where $\lambda^\star(\nu)$ satisfies the transcendental equation*

$$R_h(x_0;\lambda^\star) = -\frac{1}{2\pi\nu}\,, \qquad \nu \equiv -1/\log(\varepsilon d)\,, \qquad d = e^{-\chi(\delta_0)}\,, \tag{4.37}$$

where $\chi(\delta_0)$ is defined by (4.17b) *and is given in* (4.19) *for a circular hole of radius ε. Here, R_h is the regular part of the Helmholtz Green's function defined in* (4.36). *Since R_h is unbounded as $\lambda^\star \to \lambda_0$, it follows from* (4.37) *that $\lambda^\star \to \lambda_0$ as $\nu \to 0$, where λ_0 is an eigenvalue of* (4.12a).

As a test of Principal Result 4.2, we consider the exactly solvable case of the annulus $\varepsilon < r < 1$. By factorizing the operator $-\delta\Delta^2 + \Delta - \lambda$ as a quadratic in Δ, we find that the radially symmetric solutions of (4.2) are spanned by $\{J_0(\xi_1 r), Y_0(\xi_1 r), K_0(\xi_2 r), I_0(\xi_2 r)\}$, where

$$\xi_1 \equiv \sqrt{\frac{-1+\sqrt{1+4\delta\lambda}}{2\delta}}\,, \qquad \xi_2 \equiv \sqrt{\frac{1+\sqrt{1+4\delta\lambda}}{2\delta}}\,. \tag{4.38}$$

With the clamped boundary conditions $u_0 = \partial_r u_0 = 0$ on $r = 1$ and $r = \varepsilon$, the eigenvalues are determined

$$\det\begin{bmatrix} J_0(\xi_1) & Y_0(\xi_1) & K_0(\xi_2) & I_0(\xi_2) \\ \xi_1 J_1(\xi_1) & \xi_1 Y_1(\xi_1) & \xi_2 K_1(\xi_2) & -\xi_2 I_1(\xi_2) \\ J_0(\xi_1\varepsilon) & Y_0(\xi_1\varepsilon) & K_0(\xi_2\varepsilon) & I_0(\xi_2\varepsilon) \\ \xi_1 J_1(\xi_1\varepsilon) & \xi_1 Y_1(\xi_1\varepsilon) & \xi_2 K_1(\xi_2\varepsilon) & -\xi_2 I_1(\xi_2\varepsilon) \end{bmatrix} = 0\,. \tag{4.39}$$

To test the accuracy of Principal Result 4.2, we set $\delta = \varepsilon^2$ ($\delta_0 = 1$) in (4.38) and numerically obtain the zeros of (4.39) over a range of ε values. For the particular case $x_0 = 0$, the Helmholtz Green's function satisfying (4.36) is a linear combination $J_0(\sqrt{\lambda^\star}r)$ and $Y_0(\sqrt{\lambda^\star}r)$. The regular part $R_h(0,\lambda^\star)$ is readily calculated to be

$$R_h(0;\lambda^\star) = -\frac{1}{2\pi}\left[-\log 2 + \gamma_e + \log(\sqrt{\lambda^\star})\right] + \frac{1}{4}\frac{Y_0(\sqrt{\lambda^\star})}{J_0(\sqrt{\lambda^\star})}\,, \tag{4.40}$$

which allows for a numerical solution of the transcendental equation (4.37).

In Figure 5, a comparison of the lowest eigenvalue from the asymptotic prediction (4.37) and the exact solution shows agreement between the two theories as $\varepsilon \to 0$. In particular, the asymptotic result shows the limiting behavior $\lambda^\star \to \lambda_0$ as $\varepsilon \to 0$, where λ_0 is determined by (4.12a). For this particular example, $\lambda_0 = z_0^2 \approx 5.7832$, where $J_0(z_0) = 0$.

4.3. Weaker bi-Laplace: $\delta \ll \mathcal{O}(\varepsilon^2)$. In this subsection, we consider the case where $\delta \ll \mathcal{O}(\varepsilon^2)$. In terms of the inner variables $y = \varepsilon^{-1}(x - x_0)$ and $v(y) = u(x_0 + \varepsilon y)$, the canonical inner solution satisfies

$$-\frac{\delta}{\varepsilon^2}\Delta_y^2 v_c + \Delta_y v_c + \varepsilon^2\lambda v_c = 0\,, \qquad y \in \mathbb{R}^2 \setminus \Omega_0\,; \qquad v = \partial_n v = 0\,, \quad y \in \partial\Omega_0\,, \tag{4.41a}$$

$$v_c \sim \log|y| + \chi\,, \quad \text{as} \quad |y| \to \infty\,, \tag{4.41b}$$

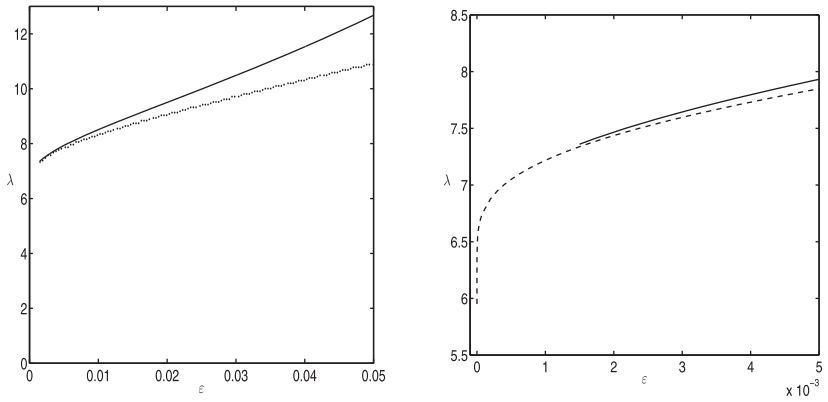

FIG. 5. *A quantitative test of Principal Result* 4.2. *The solid curve is the smallest eigenvalue calculated from the exact solution by a numerical evaluation of* (4.39). *The dotted curve is the asymptotic prediction determined from numerical solution of the transcendental equation* (4.37). *The right panel shows an enlargement for small values of* ε *and captures the limiting behavior* $\lambda^\star \to \lambda_0$ *as* $\varepsilon \to 0$.

for some constant χ to be determined. In our analysis below, where we allow Ω_0 to have an arbitrary shape, there are two regions that must be analyzed: The region where $|y| = \mathcal{O}(1)$ is called the inner region, and the range of y where $\text{dist}(y, \partial\Omega_0) = \mathcal{O}(\sqrt{\delta/\varepsilon^2}) \ll 1$ is called the subinner region.

Similar to the boundary layer analysis of section 4.1, the leading-order inner solution v_{c0} for (4.41), defined away from an $\mathcal{O}(\sqrt{\delta/\varepsilon^2})$ neighborhood of $\partial\Omega_0$, must satisfy the effective boundary condition $v_{c0} \to 0$ as $y \to \partial\Omega_0$. In the inner region, we expand v_c and χ in (4.41) as

$$v_c = v_{c0} + \sqrt{\frac{\delta}{\varepsilon^2}} v_{c1} + \cdots , \qquad \chi \sim \chi_0 + \sqrt{\frac{\delta}{\varepsilon^2}} \chi_1 + \cdots . \tag{4.42}$$

Upon substituting (4.42) into (4.41), we obtain the leading-order problem

$$\Delta v_{c0} = 0 , \quad y \in \mathbb{R}^2 \backslash \Omega_0 ; \qquad v_{c0} = 0 , \quad y \in \partial\Omega_0 , \tag{4.43a}$$

$$v_{c0} \sim \log|y| - \log d_0 , \quad \text{as} \quad |y| \to \infty ; \qquad \chi_0 \equiv -\log d_0 . \tag{4.43b}$$

In order that the term $\varepsilon^2 \lambda v_c$ appears at a lower-order than $\mathcal{O}(\sqrt{\delta/\varepsilon^2})$, we assume that $\delta \gg \mathcal{O}(\varepsilon^6)$ and obtain the problem for v_{c1}

$$\Delta v_{c1} = 0 , \quad y \in \mathbb{R}^2 \backslash \Omega_0 ; \qquad v_{c1} \sim \chi_1 , \quad \text{as} \quad |y| \to \infty . \tag{4.44}$$

In our analysis below of the subinner layer near $\partial\Omega_0$, we will derive an effective boundary condition for v_{c1} on $\partial\Omega_0$. Then, by imposing that v_{c1} is bounded as $|y| \to \infty$, we will identify the constant χ_1 in (4.44).

The PDE (4.43) is a classical problem in electrostatics (cf. [23], [20]), where the constant d_0 is referred to as the logarithmic capacitance of Ω_0. The logarithmic capacitance is known analytically for various shapes of Ω_0 (cf. [23], [20]). For the circular domain $\Omega_0 = \{y \,|\, |y| \le 1\}$, we have $v_{c0} = \log|y|$ and $d_0 = 1$.

Next, we insert a subinner layer near $\partial\Omega_0$ to satisfy the boundary condition $\partial_n v_c = 0$ on $\partial\Omega_0$. As in section 4.1, we use the orthogonal boundary-fitted coordinates

(η, s) so that (4.41) is transformed on the region $\eta \le 0$ to (see (4.3))

$$-\frac{\delta}{\varepsilon^2}\left[\partial_{\eta\eta} - \frac{\kappa_0}{1-\kappa_0\eta}\partial_\eta + \frac{1}{1-\kappa_0\eta}\partial_s\left(\frac{1}{1-\kappa_0\eta}\partial_s\right)\right]^2 v_c + \left[\partial_{\eta\eta} - \frac{\kappa_0}{1-\kappa_0\eta}\partial_\eta + \frac{1}{1-\kappa_0\eta}\partial_s\left(\frac{1}{1-\kappa_0\eta}\partial_s\right)\right] v_c + \varepsilon^2\lambda v_c = 0\,, \tag{4.45}$$

subject to $v_c = \partial_\eta v_c = 0$ on $\eta = 0$. Here, $\kappa_0 = \kappa_0(s)$ is the curvature of $\partial\Omega_0$ with $\kappa_0 = 1$ when Ω_0 is the unit disk.

We introduce the subinner layer variables $\hat\eta$ and w_c by

$$\hat\eta = \eta/\sigma\,, \qquad v_c = \sigma w_c\,, \qquad \text{where} \quad \sigma = \sqrt{\frac{\delta}{\varepsilon^2}} \ll 1\,. \tag{4.46}$$

Then, we expand $w_c = w_{c0} + \mathcal{O}(1)$ and obtain to leading-order from (4.45) that

$$-\partial_{\hat\eta\hat\eta\hat\eta\hat\eta} w_{c0} + \partial_{\hat\eta\hat\eta} w_{c0} = 0\,, \quad \hat\eta \le 0\,; \qquad w_{c0} = \partial_{\hat\eta} w_{c0} = 0\,, \quad \hat\eta = 0\,. \tag{4.47a}$$

The leading-order matching condition to the inner solution is that

$$w_{c0} \sim -\hat\eta \partial_n v_{c0}\big|_{\partial\Omega_0}\,, \quad \text{as} \quad \hat\eta \to -\infty\,, \tag{4.47b}$$

where ∂_n is the outward normal derivative to $\partial\Omega_0$. The solution to (4.47) is $w_{c0} = -\partial_n v_{c0}|_{\partial\Omega_0}[1 + \hat\eta - e^{\hat\eta}]$. In this way, the leading-order solution in the subinner region is

$$v_c \sim \sqrt{\frac{\delta}{\varepsilon^2}}\,(w_{c0} + \cdots) = -\sqrt{\frac{\delta}{\varepsilon^2}}\left[\partial_n v_{c0}\big|_{\partial\Omega_0}\left(1 + \hat\eta - e^{\hat\eta}\right) + \mathcal{O}(1)\right]\,. \tag{4.48}$$

Next, we employ a higher-order matching condition between the far-field behavior of (4.46) as $\hat\eta \to -\infty$ and the near-field behavior as $\eta \to 0$ of the inner expansion (4.42). This yields the effective boundary condition

$$v_{c1} = -\partial_n v_{c0}\big|_{\partial\Omega_0}\,, \qquad y \in \partial\Omega_0\,. \tag{4.49}$$

The problem for v_{c1} is (4.44), subject to the boundary condition (4.49) and with v_{c1} bounded as $|y| \to \infty$. To determine $\chi_1 = \lim_{|y|\to\infty} v_{c1}$, we apply Green's identity to v_{c0} and v_{c1} over the region $\Omega_L \backslash \Omega_0$, where $\Omega_L = \{y \,|\, |y| \le L\}$, and then pass to the limit $L \to \infty$. This yields that $\int_{\partial\Omega_0}(-v_{c0}\partial_n v_{c1} + v_{c1}\partial_n v_{c0})\,\mathrm{d}s = -\lim_{L\to\infty}\int_{\partial\Omega_L}(v_{c0}\partial_n v_{c1} - v_{c1}\partial_n v_{c0})\,\mathrm{d}s$. Since $v_{c0} = 0$ and $v_{c1} = -\partial_n v_{c0}$ on $\partial\Omega_0$, while $v_{c0} \sim \log L$, $v_{c1} \sim \chi_1$, and $\partial_n v_{c1} = \mathcal{O}(L^{-2})$ on $\partial\Omega_L$, we get that

$$\chi_1 = -\frac{1}{2\pi}\int_{\partial\Omega_0} (\partial_n v_{c0})^2\,\mathrm{d}s\,. \tag{4.50}$$

In this way, the two-term expansion for χ in (4.41), valid for an arbitrarily shaped hole Ω_0, is

$$\chi \sim -\log d_0 - \frac{1}{2\pi}\sqrt{\frac{\delta}{\varepsilon^2}}\int_{\partial\Omega_0} (\partial_n v_{c0})^2\,\mathrm{d}s + \cdots\,. \tag{4.51a}$$

It is then convenient to define d_δ by $\chi \equiv -\log d_\delta$ so that

$$d_\delta = e^{-\chi} \sim d_0\left(1 + \frac{1}{2\pi}\sqrt{\frac{\delta}{\varepsilon^2}}\int_{\partial\Omega_0} (\partial_n v_{c0})^2\,\mathrm{d}s\right)\,. \tag{4.51b}$$

Here, d_0 is the logarithmic capacitance of Ω_0 defined in terms of v_{c0} by (4.43). For the unit disk $\Omega_0 = \{y \,|\, |y| \le 1\}$, we have $v_{c0} = \log|y|$, $d_0 = 1$, and hence $\chi \sim -\sqrt{\delta/\varepsilon^2}$ from (4.51a). If we set $\delta = \delta_0\varepsilon^2$ in this last expression, we recover $\chi \sim -\sqrt{\delta_0}$, as was previously derived in (4.21b) of section 4.2 for the small δ_0 limit for the critical scaling regime $\delta = \delta_0\varepsilon^2$.

Finally, with d_δ determined as in (4.51b), we can then simply repeat the analysis in (4.32)–(4.36) involving the matching of the inner and outer solutions, which yields an approximation to the eigenvalue of (4.1). In place of Principal Result 4.2, we obtain the following result.

PRINCIPAL RESULT 4.3. *For $\mathcal{O}(\varepsilon^6) \ll \delta \ll \mathcal{O}(\varepsilon^2)$, there is an eigenvalue λ of (4.1) with $\lambda \sim \lambda^\star(\nu_\delta) + t.s.t$, where $\lambda^\star(\nu_\delta)$ satisfies the transcendental equation*

$$R_h(x_0;\lambda^\star(\nu_\delta)) = -\frac{1}{2\pi\nu_\delta}\,, \qquad \nu_\delta \equiv -1/\log(\varepsilon d_\delta)\,, \tag{4.52}$$

$$d_\delta \sim d_0\left(1 + \frac{1}{2\pi}\sqrt{\frac{\delta}{\varepsilon^2}}\int_{\partial\Omega_0}(\partial_n v_{c0})^2\,\mathrm{d}s\right).$$

Here, d_0 is the logarithmic capacitance of Ω_0 defined in terms of v_{c0} by (4.43), and R_h is the regular part of the Helmholtz Green's function defined in (4.36). For the unit disk $\Omega_0 = \{y \,|\, |y| \le 1\}$, we have $d_\delta \sim 1 + \sqrt{\delta/\varepsilon^2}$.

We remark that the leading-order term $d_\delta \sim d_0$ still holds even without the extra technical restriction that $\delta \gg \mathcal{O}(\varepsilon^6)$. Using the leading-order result $d_\delta \sim d_0$, Principal Result 4.3 shows that when $\delta \ll \mathcal{O}(\varepsilon^2)$, the approximation to the eigenvalue for (4.1) is the same to within all logarithmic terms as that for an eigenvalue of the Laplacian in a domain with a hole, as analyzed in [23]. The second-order term for d_δ in (4.52) characterizes the weak influence on $\lambda^\star$ of the fourth-order term $-\delta\Delta^2$ in the regime $\mathcal{O}(\varepsilon^6) \ll \delta \ll \mathcal{O}(\varepsilon^2)$ for an arbitrarily shaped hole.

4.4. Stronger bi-Laplace: $\mathcal{O}(\varepsilon^2) \ll \delta \ll \mathcal{O}(1)$. Next, we consider the range $\mathcal{O}(\varepsilon^2) \ll \delta \ll \mathcal{O}(1)$. In terms of the inner variable $y = \varepsilon^{-1}(x - x_0)$ and $v(y) = u(x_0 + \varepsilon y)$, the canonical inner solution still satisfies (4.41). In our analysis, there are two regions that must be analyzed: an inner region with $|y| = \mathcal{O}(1)$, where Δ^2 dominates in (4.41), and a far-inner region with $z = y/(\sqrt{\delta}/\varepsilon) = \mathcal{O}(1)$, where $-\Delta^2$ and Δ balance in (4.41). We will first consider the special case of a circular hole where $\Omega_0 = \{y \,|\, |y| \le 1\}$.

In the far-inner region, we introduce the local variables z and w_c, and we obtain to leading order from (4.41) that

$$-\Delta_z^2 w_{c0} + \Delta w_{c0} = 0\,, \qquad |z| \ge 0\,. \tag{4.53}$$

We look for a radially symmetric solution to (4.53) satisfying $w_{c0} \sim \log|z|$ as $|z| \to \infty$ and $w_{c0} \to 0$ as $|z| \to 0$. The necessity of this second condition, which allows for an asymptotic matching of w_{c0} as $|z| \to 0$ with the far-field behavior of the leading-order inner solution, is discussed in Remark 1. Any radially symmetric solution to (4.53) is a linear combination of $\{1, \log|z|, K_0(|z|), I_0(|z|)\}$. Upon using the asymptotics (4.20) for $K_0(|z|)$ as $|z| \to 0$, it readily follows that the solution to (4.53) that satisfies $w_{c0} \sim \log|z|$ as $z \to \infty$ and $w_{c0} \to 0$ as $|z| \to 0$ is

$$w_{c0} = \gamma_e - \log 2 + \log|z| + K_0(|z|)\,. \tag{4.54}$$

Upon using (4.20), we obtain the more refined behavior

$$w_{c0} \sim -\frac{1}{4}|z|^2 \log|z| + \frac{|z|^2}{4}\left(\log 2 + 1 - \gamma_e\right), \quad \text{as} \quad |z| \to 0\,. \tag{4.55}$$

In terms of the inner variable y, defined by $z = y/(\sqrt{\delta}/\varepsilon)$, (4.55) then yields

$$w_{c0} \sim -\frac{|y|^2}{4}\frac{\varepsilon^2}{\delta}\log\left(\frac{\varepsilon}{\sqrt{\delta}}\right) + \frac{\varepsilon^2}{4\delta}\left[-|y|^2\log|y| + |y|^2\left(\log 2 + 1 - \gamma_e\right)\right] + \cdots . \tag{4.56}$$

The matching condition is that the far-field behavior as $|y| \to \infty$ of the inner solution must agree with (4.56).

Motivated by (4.56), which suggests the asymptotic gauge functions, the inner solution for (4.41) is expanded as

$$v_c \sim \left(-\frac{\varepsilon^2}{\delta}\log\left(\frac{\varepsilon}{\sqrt{\delta}}\right)\right) v_{c0} + \frac{\varepsilon^2}{\delta} v_{c1} + \cdots . \tag{4.57}$$

Upon substituting (4.57) into (4.41), and by using the matching condition (4.56), we obtain that the radially symmetric functions $v_{c0}(|y|)$ and $v_{c1}(|y|)$ satisfy

$$\Delta_y^2 v_{c0} = 0 \quad \text{in} \quad |y| \ge 1\,; \qquad v_{c0} = v_{c0}' = 0 \quad \text{on} \quad |y| = 1\,; \qquad v_{c0} \sim |y|^2/4\,, \quad \text{as} \quad |y| \to \infty \tag{4.58a}$$

and

$$\Delta_y^2 v_{c1} = 0 \quad \text{in} \quad |y| \ge 1\,; \qquad v_{c1} = v_{c1}' = 0 \quad \text{on} \quad |y| = 1\,, \tag{4.58b}$$

$$v_{c1} \sim -\frac{|y|^2}{4}\log|y| + \frac{|y|^2}{4}\left(\log 2 + 1 - \gamma_e\right), \quad \text{as} \quad |y| \to \infty\,. \tag{4.58c}$$

These two problems can be solved explicitly to obtain

$$v_{c0} = \frac{1}{4}\left(|y|^2 - 1\right) - \frac{1}{2}\log|y|\,; \quad v_{c1} = \frac{1}{4}\left(\log 2 + 1 - \gamma_e\right)\left(|y|^2 - 1\right) - \frac{|y|^2}{4}\log|y| - \left(\frac{1}{2}\log 2 + \frac{1}{4} - \frac{\gamma_e}{2}\right)\log|y|\,. \tag{4.59}$$

Remark 1. The condition $w_{c0} \to 0$ as $|z| \to 0$ for the solution (4.53) is required in order to match to the inner solution. If, instead, $w_{c0} \to A \neq 0$ as $|z| \to 0$, then in the inner region we would expand $v_c \sim v_{c0}(|y|) + o(1)$ to obtain the leading-order problem $\Delta_y^2 v_{c0} = 0$ in $|y| \ge 1$ with $v_{c0} = v_{c0}' = 0$ on $|y| = 1$ with $v_{c0} \to A$ as $|y| \to \infty$. Since v_{c0} is a linear combination of $\{1, \log|y|, |y|^2, |y|^2\log|y|\}$, there is no such solution when $A \neq 0$.

Next, to determine the matching behavior as $x \to x_0$ required for the outer solution, we let $|z| \to \infty$ in (4.54), and we write the resulting expression in terms of y using $|z| = y/(\sqrt{\delta}/\varepsilon)$. This yields that

$$v_c \sim \log|y| - \log d_\infty + o(1)\,, \quad \text{as} \quad |y| \to \infty\,; \qquad d_\infty \equiv \frac{2\sqrt{\delta}}{\varepsilon}e^{-\gamma_e}\,. \tag{4.60}$$

With the far-field behavior of the solution to (4.41) now known for the regime $\mathcal{O}(\varepsilon^2) \ll \delta \ll 1$, we then simply repeat the analysis in (4.32)–(4.36) for the matching to the outer solution. This leads to the following result.

Principal Result 4.4. *Consider* (4.1) *with a circular hole of radius* ε *centered at* $x = x_0$ *for the range* $\mathcal{O}(\varepsilon^2) \ll \delta \ll \mathcal{O}(1)$. *Then, there is an eigenvalue* λ *of* (4.1)

with $\lambda \sim \lambda^\star(\nu_\infty)$, where $\lambda^\star(\nu_\infty)$ satisfies the transcendental equation

$$R_h(x_0;\lambda^\star) = -\frac{1}{2\pi\nu_\infty}\,, \qquad \nu_\infty \equiv -1/\log\left(2\sqrt{\delta}e^{-\gamma_e}\right). \tag{4.61}$$

Here, R_h is the regular part of the Helmholtz Green's function defined in (4.36) *and γ_e is Euler's constant.*

The central implication of this result is that on the range $\mathcal{O}(\varepsilon^2) \ll \delta \ll \mathcal{O}(1)$, the approximation $\lambda^\star$ to the eigenvalue is independent of the radius ε of the hole and depends on δ, the hole location x_0, and the shape of Ω. Therefore, we state that it is in this asymptotic range of δ where the asymptotic result for λ provides a smooth transition to the result obtained in section 3 involving a point constraint. More precisely, the result (4.61) was previously obtained in (3.15) from formally taking the small δ limit of the point constraint formulation of section 3. Alternatively, if we formally set $\delta = \varepsilon^2\delta_0$ in (4.61), we recover the same limiting expression as that obtained by letting $\delta_0 \gg 1$ in the asymptotic result (4.37) of Principal Result 4.2 derived for the critical scaling regime $\delta = \mathcal{O}(\varepsilon^2)$.

Although (4.61) does provide the leading asymptotic behavior as $\delta \to 0$, the example below for the annulus shows that it is not particularly accurate for moderately small δ. The discrepancy at moderately small values of δ arises from neglecting the boundary layer of width $\mathcal{O}(\delta^{1/2})$ in the vicinity of $\partial\Omega$ in which the clamped boundary conditions (1.3b) are satisfied. For an arbitrary domain with smooth boundary, we now extend the analysis leading to Principal Result 4.4 to account for the boundary layer near $\partial\Omega$. Motivated by the analysis in section 4.1, we substitute the expansion

$$u = u^\star(x,\nu_\infty) + \delta^{1/2}u_1(x,\nu_\infty) + \cdots\,, \qquad \lambda = \lambda^\star(\nu_\infty) + \delta^{1/2}\lambda_1(\nu_\infty) + \cdots \tag{4.62}$$

into (1.3) and equate powers of $\delta^{1/2}$. At leading order, $(\lambda^\star, u^\star)$ satisfy (4.34), with normalization condition $\int_\Omega [u^\star]^2\,\mathrm{d}x = 1$, while the pair (λ_1, u_1) satisfies

$$\Delta u_1 + \lambda^\star u_1 = -\lambda_1 u^\star\,, \quad x \in \Omega\backslash\{x_0\}\,; \qquad u_1 = \partial_n u^\star\,, \quad x \in \partial\Omega\,; \qquad \int_\Omega u_1 u^\star\,\mathrm{d}x = 0\,. \tag{4.63}$$

The boundary condition for u_1 on $\partial\Omega$ in (4.63) arises from a similar boundary layer analysis as in section 4.1 (see (4.12b)).

To establish a condition that fixes λ_1, the singular behavior of u_1 as $x \to x_0$ is obtained by writing $u_1 = A_1(\nu_\infty)\nu_\infty v_c(|y|)$ in the inner region. Using the established behavior of v_c in (4.60), we have that u_1 must satisfy

$$u_1 \sim A_1\nu_\infty \log|x - x_0| + A_1\,, \quad \text{as} \quad x \to x_0\,. \tag{4.64}$$

We then decompose $u_1 = u_{1p} + u_{1s}$, where u_{1p} is a smooth particular solution and u_{1s} is a solution that is singular as $x \to x_0$. The local behavior (4.64) indicates that $u_{1s} = -2\pi A_1\nu_\infty G_h(x;x_0,\lambda^\star)$, leaving u_{1p} to solve

$$\Delta u_{1p} + \lambda^\star u_{1p} = -\lambda_1 u^\star\,, \quad x \in \Omega\,; \qquad u_{1p} = \partial_n u^\star\,, \quad x \in \partial\Omega\,. \tag{4.65}$$

The local behavior of the decomposed solution as $x \to x_0$ is obtained by using (4.36b) and the fact that u_{1p} is smooth for all $x \in \Omega$. This yields

$$u_1 \sim u_{1p}(x_0) + A_1\nu_\infty \log|x - x_0| - 2\pi A_1\nu_\infty R_h(x_0,\lambda^\star) + o(1), \qquad x \to x_0\,. \tag{4.66}$$

Upon comparing (4.66) and (4.64), and noting that $-2\pi\nu_\infty R_h(x_0,\lambda^\star)=1$ from (4.61), we conclude that $u_{1p}(x_0)=0$. We now show that this condition determines λ_1. By applying Green's identity to u_{1p} and G_h, we derive

$$\int_\Omega \left[u_{1p}(\Delta G_h+\lambda^\star G_h)-G_h(\Delta u_{1p}+\lambda^\star u_{1p})\right]\,\mathrm{d}x=\int_{\partial\Omega}\left(u_{1p}\partial_n G_h-G_h\partial_n u_{1p}\right)\,\mathrm{d}s\,.$$

Upon substituting (4.63) and (4.36) into this identity, we obtain that $-u_{1p}(x_0)+\lambda_1\int_\Omega u^\star G_h\,\mathrm{d}x=\int_{\partial\Omega}\left(\partial_n u^\star\right)\left(\partial_n G_h\right)\,\mathrm{d}s$. Finally, applying the condition $u_{1p}(x_0)=0$ and recalling from (4.35) that $u^\star=-2\pi\,\mathcal{C}G_h(x;x_0,\lambda^\star)$, we conclude that

$$\lambda_1=\frac{\displaystyle\int_{\partial\Omega}(\partial_n G_h)^2\,\mathrm{d}s}{\displaystyle\int_\Omega (G_h)^2\,\mathrm{d}x}\,. \tag{4.67}$$

The constant A_1 is $A_1=-\left[2\pi\nu_\infty\right]^{-1}\int_\Omega G_h u_{1p}\,\mathrm{d}x/\int_\Omega G_h^2\,\mathrm{d}x$, which results from imposing the normalization condition $\int_\Omega u^\star u_1\mathrm{d}x=0$. We summarize the result as follows.

Principal Result 4.5. *Consider* (4.1) *with a circular hole of radius* ε *centered at* $x=x_0$ *for the range* $\mathcal{O}(\varepsilon^2)\ll\delta\ll\mathcal{O}(1)$. *Then, there is an eigenvalue* λ *of* (4.1) *with*

$$\lambda\sim\lambda^\star(\nu_\infty)+\delta^{1/2}\lambda_1(\nu_\infty)+\cdots\,, \tag{4.68}$$

where $\lambda^\star(\nu_\infty)$ *satisfies the transcendental equation* (4.61), *and* λ_1 *is given in* (4.67).

As a test of the accuracy of Principal Result 4.5, we revisit the case considered at the end of section 4.2 where Ω is the annular domain $\varepsilon<r<1$, for which closed form solutions are available. The exact eigenvalues are determined by (4.39), which are solved numerically. To implement the asymptotic theory, we recall that R_h is given in (4.40). In addition, by calculating G_h analytically from (4.36), we determine λ_1 in (4.67) as

$$\lambda_1(\nu_\infty)=\frac{4}{\pi^2}\left(\int_0^1 r\Big[Y_0(\sqrt{\lambda^\star(\nu_\infty)}r)J_0(\sqrt{\lambda^\star(\nu_\infty)})-Y_0(\sqrt{\lambda^\star(\nu_\infty)})J_0(\sqrt{\lambda^\star(\nu_\infty)}r)\Big]^2\,\mathrm{d}r\right)^{-1}. \tag{4.69}$$

As $\delta\to0$, for which $\lambda^\star\to\lambda_0$, where λ_0 is an eigenvalue of the Laplacian, (4.69) readily reduces upon using the Wronskian relation between J_0 and Y_0 to $\lambda_1\to2\lambda_0$. A similar boundary layer correction term can be added to the result for $\lambda^\star$ in (4.37) of Principal Result 4.2 that is valid when $\delta=\mathcal{O}(\varepsilon^2)$. This leads to the approximation

$$\lambda\sim\lambda^\star(\nu)+\delta^{1/2}\lambda_1(\nu)+\cdots\,. \tag{4.70}$$

Here, $\lambda^\star(\nu)$ and ν are defined in (4.37) and λ_1 is obtained by replacing ν_∞ in (4.69) with ν.

For a circular hole with radius $\varepsilon=0.01$, in Figure 6 we show a reasonably favorable comparison over a range of values of δ between the asymptotic results (4.68) and (4.70) for the lowest eigenvalue and the exact result, as obtained by solving (4.39) numerically. From the insert in this figure, we observe that (4.70) provides a more

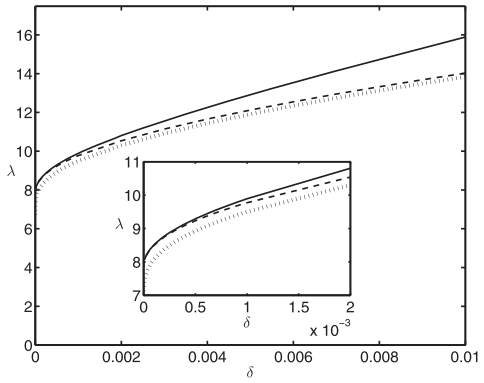

FIG. 6. *Comparison of the asymptotic result* (4.68) *for the lowest eigenvalue* λ *versus* δ *(dotted curve) and the exact result (solid curve), as obtained by solving* (4.39) *numerically, for an annular domain* $\varepsilon \le |x| \le 1$ *with* $\varepsilon = 0.01$. *The dashed curve is the asymptotic result* (4.70) *that represents adding a boundary layer correction term to the result for* $\lambda^\star(\nu)$ *of Principal Result* 4.2 *that applies for the regime* $\delta = \mathcal{O}(\varepsilon^2)$. *As expected, this latter result is more accurate than* (4.68) *when* δ *is small, and it tends to the result in* (4.68) *as* δ *is increased.*

accurate prediction than (4.68) when δ is small and that the results in (4.70) and (4.68) are essentially indistinguishable for larger δ. However, neither approximation is particularly accurate when $\delta \approx 0.01$. The reason for the discrepancy is likely due to not including higher-order boundary layer contributions of order $\mathcal{O}(\delta)$. In fact, from (4.13), one of the terms of $\mathcal{O}(\delta)$ is $\lambda_0^2\delta$, which is quantitatively significant even when $\delta = 0.01$.

We remark that, although we have derived Principal Results 4.4 and 4.5 only for the case of a circular hole, these results still hold for an arbitrarily shaped hole Ω_0. Therefore, the effect of the hole shape on the eigenvalue on the range $\mathcal{O}(\varepsilon^2) \ll \delta \ll \mathcal{O}(1)$ is only through higher-order correction terms to (4.61) and (4.68). To show this, we observe that the leading-order solution for the far-inner region still holds, which in turn motivates the inner expansion (4.57). For an arbitrarily shaped hole, and in place of (4.58), the nonradially symmetric functions v_{c0} and v_{c1} now satisfy

$$\Delta_y^2 v_{c0} = 0\,, \quad y \in \mathbb{R}^2\backslash\Omega_0\,; \qquad v_{c0} = \partial_n v_{c0} = 0\,, \quad y \in \partial\Omega_0\,, \tag{4.71a}$$

$$v_{c0} \sim |y|^2/4\,, \quad \text{as} \quad |y| \to \infty\,, \tag{4.71b}$$

$$\Delta_y^2 v_{c1} = 0\,, \quad y \in \mathbb{R}^2\backslash\Omega_0\,; \qquad v_{c1} = \partial_n v_{c1} = 0\,, \quad y \in \partial\Omega_0\,, \tag{4.71c}$$

$$v_{c1} \sim -\frac{|y|^2}{4}\log|y| + \frac{|y|^2}{4}\left(\log 2 + 1 - \gamma_e\right)\,, \quad \text{as} \quad |y| \to \infty\,. \tag{4.71d}$$

Since the solutions of the homogeneous problem for v_{ck} for $k = 0, 1$ are linear combinations of $\{\rho^2\log\rho, \rho^2, \log\rho, 1\}$, $\{\rho^3, \rho\log\rho, \rho, \rho^{-1}\} \times \{\cos\theta, \sin\theta\}$, and $\{\rho^4, \rho^2, 1, \rho^{-2}\} \times \{\cos 2\theta, \sin 2\theta\}$, etc., where $y = \rho(\cos\theta, \sin\theta)$ and $\rho = |y|$, the far-field behavior of the solution v_0 to (4.71) must have the form

$$v_{c0} \sim \frac{1}{4}|y|^2 + A_0\log|y| + f_0\cdot y + \frac{y^T\mathcal{D}_0 y}{|y|^2} + o(1)\,, \quad \text{as} \quad |y| \to \infty \tag{4.72}$$

for some constant A_0, vector f_0, and matrix $\mathcal{D}_0$, all determined by the shape of Ω_0. Notice that we have imposed that $|y|^{-1}(v_{c0} - |y|^2/4)$ is bounded as $|y| \to \infty$. In contrast, for v_{c1} we must allow for a growth of order $\mathcal{O}(y\log|y|)$ as $|y| \to \infty$. In terms

of an arbitrary vector b_1, the far-field behavior of this solution to (4.71) has the form

$$v_{c1} \sim -\frac{1}{4}|y|^2 \log|y| + \frac{|y|^2}{4}(\log 2 + 1 - \gamma_e) + b_1 \cdot y \log|y| + f_1 \cdot y + A_1 \log|y| + \frac{y^T \mathcal{D}_1 y}{|y|^2} + o(1), \quad \text{as} \quad |y| \to \infty \tag{4.73}$$

for some constant A_1, vector f_1, and matrix $\mathcal{D}_1$ determined in terms of the unknown b_1 and the shape of Ω_0. We remark that the unknown vector b_1 is eventually determined by the gradient of the regular part of the Helmholtz Green's function at $x = x_0$. The terms A_j, f_j, $\mathcal{D}_j$ for $j = 0, 1$ then induce new higher-order nonradially symmetric correction terms to the far-inner solution. However, it is clear that the effect of these terms on the eigenvalue is of negligible asymptotic order as compared to (4.61).

5. A numerical experiment. In this section, we illustrate Principal Results 4.4 and 4.5 for the case where Ω is the unit disk with an off-centered hole of radius ε centered at $x_0 \in \Omega$. We will consider the parameter regime where $\mathcal{O}(\varepsilon^2) \ll \delta \ll \mathcal{O}(1)$.

We first must determine the regular part $R_h(x_0; \lambda^\star)$ of the Helmholtz Green's function defined in (4.36). Set $x = r(\cos\theta, \sin\theta)$ and suppose without loss of generality that $x_0 = (r_0, 0)$. A standard Fourier series expansion of the solution to (4.36) yields

$$G_h(x_0; \lambda^\star) = -\frac{1}{4} J_0(r_< c)\left(Y_0(r_> c) - J_0(r_> c)\frac{Y_0(c)}{J_0(c)}\right) - \frac{1}{2}\sum_{m=1}^{\infty} \cos(m\theta) J_m(r_< c)\left(Y_m(r_> c) - J_m(r_> c)\frac{Y_m(c)}{J_m(c)}\right), \tag{5.1}$$

where we have defined $r_<$, $r_>$, and c by

$$r_< \equiv \min(r, r_0), \qquad r_> \equiv \max(r, r_0), \qquad c \equiv \sqrt{\lambda^\star}.$$

Similarly, the Fourier series expansion of the free-space Green's function is

$$\log|x - x_0| = \log r_> - \sum_{m=1}^{\infty} \frac{1}{m}\left(\frac{r_<}{r_>}\right)^m \cos(m\theta). \tag{5.2}$$

By combining (5.1) and (5.2), and noting the singularity behavior in (4.36), we identify R_h as

$$R_h(x_0; \lambda^\star) = \frac{1}{2\pi}\log r_0 - \frac{1}{4} J_0(r_0 c)\left(Y_0(r_0 c) - J_0(r_0 c)\frac{Y_0(c)}{J_0(c)}\right) + \sum_{m=1}^{\infty}\left\{-\frac{1}{2\pi m} - \frac{1}{2} J_m(r_0 c)\left(Y_m(r_0 c) - J_m(r_0 c)\frac{Y_m(c)}{J_m(c)}\right)\right\}. \tag{5.3}$$

The series in (5.3) is convergent, as can be seen by using the large-m asymptotics $J_m(r) \sim \frac{(r/2)^m}{\Gamma(m+1)}(1 + O(1/m))$, $Y_m(r) \sim (r/2)^{-m}\Gamma(m)(1 + O(1/m))$, so that for large m, the terms of the sum in (5.3) behave like $O(1/m^2)$.

From Principal Result 4.4, $\lambda^\star$ is a root of the transcendental equation

$$R_h(x_0;\ \lambda^\star) = \frac{1}{2\pi}\log\left(2\sqrt{\delta} e^{-\gamma}\right). \tag{5.4}$$

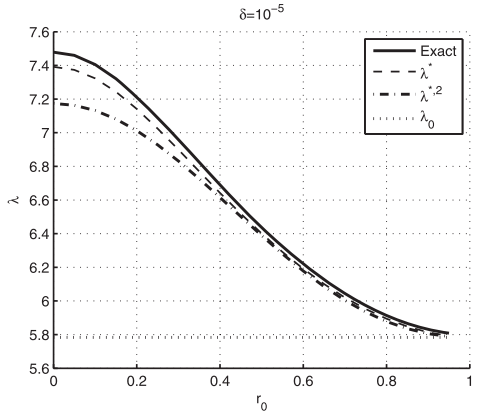

FIG. 7. *For $\delta = 10^{-5}$ and hole radius $\varepsilon = 0.001$, we compare the one-term $\lambda \sim c_0^2$, two-term* (5.6)*, and hybrid approximation* (5.4) *for the lowest eigenvalue of* (4.1) *with the corresponding "exact" result as obtained by solving* (4.1) *numerically. The domain is the unit disk with an off-centered hole at distance r_0 from the origin.*

We seek to determine the lowest root of (5.4). First, consider the case where r_0 is small. Using the small-r expansions $J_m(r) \sim r^m 2^{-m}/\Gamma(1+m)$, $m > 0$, and $Y_m(r) \sim -r^m 2^m \Gamma(m)/\pi$, $m > 0$, one readily sees that the sum in (5.3) tends to zero as $r_0 \to 0$. Using the small-r asymptotics of $Y_0(r) \sim 2/\pi(\ln r - \ln 2 + \gamma)$ and $J_0(r) \sim 1$, we readily obtain that

$$R_h(x_0, \lambda^\star) \sim \frac{1}{2\pi}\left(\log 2 - \gamma - \log c\right) + \frac{1}{4}\frac{Y_0(c)}{J_0(c)}\,, \qquad |x_0| \ll 1\,.$$

Therefore, for $x_0 = 0$, (5.4) reduces to

$$-\log c + \frac{\pi}{2}\frac{Y_0(c)}{J_0(c)} = \frac{1}{2}\log\delta\,. \tag{5.5}$$

More generally, for $|x_0| \neq 0$, expanding (5.4) to two orders yields the following two-term approximation $\lambda^{\star,2}$ to $\lambda^\star$:

$$\sqrt{\lambda^{\star,2}} \sim c_0 + \frac{\pi}{\log\left(2e^{-\gamma}\sqrt{\delta}\right)}\frac{J_0^2\left(c_0 r_0\right) Y_0(c_0)}{2J_0'(c_0)}\,. \tag{5.6}$$

Here, $c_0 \approx 2.4048$ is the first root of $J_0(c_0) = 0$.

For $\delta = 10^{-5}$ and hole radius $\varepsilon = 0.001$, in Figure 7 we compare the one-term $\lambda \sim c_0^2$, two-term (5.6), and hybrid approximation (5.4) for the lowest eigenvalue of the (4.1) with the corresponding "exact" result as obtained by solving (4.1) numerically. The hybrid result is seen to provide a decent approximation to the eigenvalue.

Next, we show how to calculate the coefficient λ_1, given in (4.67) as needed in Principal Result 4.5. Upon using the Wronskian relation in (5.1), we calculate the numerator in (4.67) as

$$\int_{\partial\Omega}\left(\partial_n G\right)^2 \mathrm{d}s = \frac{1}{2\pi}\sum_{m=0}^{\infty}\left[\frac{J_m\left(cr_0\right)}{J_m(c)}\right]^2\,. \tag{5.7}$$

TABLE 1

For a single hole of radius $\varepsilon = \sqrt{\delta/100}$, we compare the asymptotic and numerical results for the lowest eigenvalue of (4.1) for various values of δ and r_0, where r_0 is the distance of the hole from the center of the unit disk. The third column is the full numerical result, the fourth column $\lambda^\star$ is the solution to (5.4), the fifth column is the boundary layer correction term λ_1 in (4.67), while the sixth column is the asymptotic approximation $\lambda \sim \lambda^\star + \sqrt{\delta}\lambda_1$, which includes the boundary layer correction term.

r_0	δ	λ_{exact}	$\lambda^\star$	λ_1	$\lambda^\star + \sqrt{\delta}\lambda_1$	$(\lambda_{exact} - \lambda^\star)/\sqrt{\delta}$
0	0.0001	8.106	7.912	16.418	8.076	19.430
0	1e-05	7.443	7.391	15.126	7.439	16.346
0	1e-06	7.088	7.073	14.369	7.087	15.118
0.2	0.0001	7.718	7.545	14.740	7.692	17.267
0.2	1e-05	7.188	7.141	14.022	7.185	14.650
0.2	1e-06	6.898	6.885	13.557	6.899	13.020
0.5	0.0001	6.693	6.563	11.625	6.679	12.936
0.5	1e-05	6.434	6.400	11.630	6.437	10.734

Next, we compute the denominator in (4.67) as

$$\int_\Omega G^2 \,\mathrm{d}x = \frac{\pi}{2} \sum_{m=0}^{\infty} \int_0^1 \left(J_m\left(cr_<\right) Z_m\left(cr_>; m\right)\right)^2 r \,\mathrm{d}r\,, \tag{5.8}$$

$$\text{where} \qquad Z_m(x;n) \equiv Y_m\left(x\right) - J_m(x)\frac{Y_n(c)}{J_n(c)}\,.$$

Then, by using the indefinite integral (cf. [13] formula 5.54)

$$\int B_m^2(cr) r \,\mathrm{d}r = \frac{r^2}{2}\left(B_m^2(cr) - B_{m-1}(cr)B_{m+1}(cr)\right)\,, \tag{5.9}$$

where B is any Bessel function, we obtain, after some simplifications, that

$$\begin{aligned}
&\int_0^1 \left(J_m\left(cr_<\right) Z_m\left(cr_>; m\right)\right)^2 r\mathrm{d}r \\
&\quad = J_m^2(cr_0)\left[\frac{r_0^2}{2} Z_{m-1}(cr_0;m)Z_{m+1}(cr_0;m) + \frac{1}{2} Z_{m-1}(c;m)Z_{m+1}(c;m)\right] \\
&\qquad - \frac{r_0^2}{2} Z_m^2(cr_0;m)J_{m-1}(cr_0)J_{m+1}(cr_0).
\end{aligned}$$

This allows us to compute the denominator in (4.67).

In Table 1, we give some full numerical results for the lowest eigenvalue of (4.1). The computations were done assuming a hole radius of $\varepsilon = \sqrt{\delta/100}$. These "exact" results are then compared with the asymptotic result $\lambda \sim \lambda^\star$ and the improved asymptotic result $\lambda \sim \lambda^\star + \sqrt{\delta}\lambda_1$, which adds the boundary layer correction term. From this table, we observe that the improved asymptotic result agrees very favorably with the full numerical result. In each of the following examples, the "exact" results are obtained by means of finite element simulation [11] of the full problem (4.1).

In Figure 8, we apply Principal Result 4.5 to the case of the disk but with the perturbing hole centered away from the origin. The inclusion of the $\delta^{1/2}\lambda^\star$ boundary correction term improves the accuracy of the expansion dramatically, even when δ is moderately small. The full numerical simulations of (4.1) with an off centered hole are obtained from finite element simulation [11].

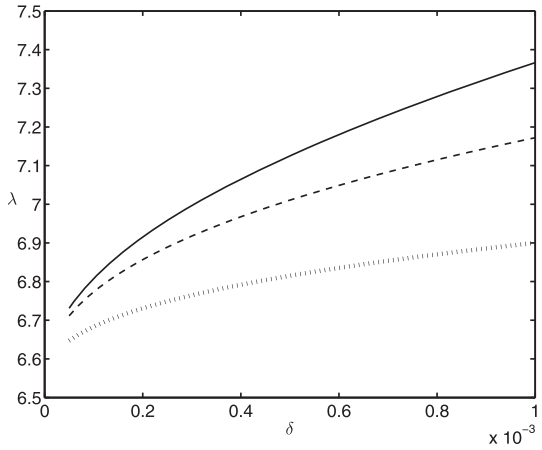

FIG. 8. *Application of Principal Result* 4.5 *for the case of a hole at* $x_0 = (0.5, 0)$ *with radius* $\varepsilon = 0.01$. *The solid line is from full numerical simulation of* (4.1) *together with the leading-order term (dotted line) and two term (dashed line) of the expansion* (4.68).

6. Discussion. We have analyzed the limiting asymptotic behavior of the mixed eigenvalue problem (4.1) in the dual limit $\varepsilon \to 0$ and $\delta \to 0$. Our analysis has identified the following three key parameter regimes, where different eigenvalue asymptotics occur: $\delta = \mathcal{O}(\varepsilon^2)$, $\delta \ll \mathcal{O}(\varepsilon^2)$, and $\mathcal{O}(\varepsilon^2) \ll \delta \ll 1$. In the regime $\mathcal{O}(\varepsilon^2) \ll \delta \ll 1$, we have shown in Principal Result 4.4 that the leading-order asymptotic behavior of an eigenvalue of (4.1) is asymptotically independent of ε. As a result, this regime provides a transition to the point constraint problem associated with the $\delta = \mathcal{O}(1)$ regime. Results from the asymptotic theory were favorably compared with full numerical results.

There are several directions that warrant further investigation. First, by developing a boundary integral method to compute $\chi(\delta_0)$ numerically for an arbitrarily shaped hole from the canonical inner problem (4.17) that holds for the scaling regime $\delta = \mathcal{O}(\varepsilon^2)$, Principal Result 4.2 could then be readily implemented for general hole shapes. In this paper, $\chi(\delta_0)$ has been determined analytically only for a circular-shaped hole.

A second, more fundamental, open direction would be to analyze (4.1) for the regime $\delta = \mathcal{O}(1)$ in the presence of $N \geq 1$ holes of asymptotically small radii $\mathcal{O}(\varepsilon) \ll 1$. In the limit $\varepsilon \to 0$, and for $\delta = \mathcal{O}(1)$, an eigenvalue λ_ε of the perturbed problem tends to an eigenvalue λ_0 of the limiting point constraint problem

$$-\delta\Delta^2 u_0 + \Delta u_0 + \lambda_0 u = 0\,, \quad x \in \Omega\,; \qquad \int_{\Omega\setminus\Omega_\varepsilon} u_0^2\,\mathrm{d}x = 1\,, \tag{6.1a}$$

$$u_0 = \partial_n u_0 = 0\,, \quad x \in \partial\Omega\,; \qquad u_0(x_j) = 0\,, \quad j = 1\ldots, N\,, \tag{6.1b}$$

where x_j for $j = 1, \ldots, N$ are the centers of the small holes. It would be interesting to develop a numerical method to compute the eigenvalues λ_0 of this point constraint problem and to determine how they depend on δ, with $\delta = \mathcal{O}(1)$, and the hole locations. In particular, where should the centers of N holes be located so as to minimize the principal eigenvalue of the limiting point constraint problem (6.1)? In the unit disk, optimal configurations of small holes that minimize the principal eigenvalue of the Laplacian in a two-dimensional domain Ω with Neumann boundary condition on

$\partial\Omega$ and with a homogeneous Dirichlet boundary condition on each of the N holes were identified in [14]. For $\delta = \mathcal{O}(1)$ and for the case of multiple small holes, it would also be interesting to extend the analysis of [5] and [15], valid for a one hole pattern for the pure biharmonic operator, to determine ε-dependent correction terms for the difference $\lambda_\varepsilon - \lambda_0$.

Finally, it would be interesting to analyze localization behavior for the eigenfunctions u_0 of the point constraint problem (6.1). For the pure biharmonic eigenvalue defined in a thin rectangular domain, and with a clamped point, the numerical computations in [10] showed that almost all of the eigenfunctions of the point constraint problem are typically confined to one side of a vertical line parallel to the thin edge of the rectangle that goes through the clamped point. In this way, the existence of a clamped point in the domain has a large effect on the geometric patterns and localization behavior of the eigenfunctions. It would be interesting to extend this analysis of [10] to (4.1).

REFERENCES

[1] M. Abramowitz and I. Stegun, *Handbook of Mathematical Functions*, 9th ed., Dover Publications, New York, 1965.

[2] C. Alves and P. Antunes, *The method of fundamental solutions applied to the calculation of eigensolutions for* 2*D plates*, Internat. J. Numer. Methods. Engrg., 77 (2009), pp. 177–194.

[3] I. V. Andrianov, V. V. Danishevs'kyy, and A. L. Kalamkarov, *Asymptotic analysis of perforated plates and membranes. Part* 1: *Static problems for small holes*, Int. J. Solids and Structures., 49 (2012), pp. 298–310.

[4] K. A. Burgemeister and C. H. Hansen, *Calculating resonant frequencies of perforated plates*, J. Sound Vibrat., 196 (1996), pp. 387–399.

[5] A. Campbell and S. A. Nazarov, *Asymptotics of eigenvalues of a plate with a small clamped zone*, Positivity, 5 (2001), pp. 275–295.

[6] G. Chardon and L. Daudet, *Low-complexity computation of plate eigenmodes with Vekua approximations and the method of particular solutions*, Comput. Mech., 52 (2013), pp. 983–992.

[7] S. Choi, H. Jeong, T. Kim, K. Kim, and K. Park, *Free vibration analysis of perforated plates using equivalent elastic properties*, J. Korean Nuclear Soc., 30 (1998), pp. 416–423.

[8] C. V. Coffman and R. J. Duffin, *On the fundamental eigenfunctions of a clamped punctured disk*, Adv. Appl. Math., 13 (1992), pp. 142–151.

[9] C. V. Coffman, R. J. Duffin, and D. H. Shaffer, *The fundamental mode of vibration of a clamped annular plate is not of one sign*, Constructive Approaches to Mathematical Models, Academic Press, New York, 1979, pp. 267–277.

[10] M. Filoche and S. Mayboroda, *Strong localization induced by one clamped point in thin plate vibrations*, Phys. Rev. Lett., 103 (2009), 254301.

[11] FlexPDE6, *PDE Solutions*, http://www.pdesolutions.com.

[12] M. Flucher, *Approximation of Dirichlet eigenvalues on domains with small holes*, J. Math. Anal. Appl., 193 (1995), pp. 169–199.

[13] I. S. Gradshteyn and I. M. Ryzhik, *Tables on Integrals, Series, and Products*, Academic Press, New York, 1965.

[14] T. Kolokolnikov, M. Titcombe, and M. J. Ward, *Optimizing the fundamental Neumann eigenvalue for the Laplacian in a domain with small traps*, European J. Appl. Math., 16 (2005), pp. 161–200.

[15] M. C. Kropinski, A. E. Lindsay, and M. J. Ward, *Asymptotic analysis of localized solutions to some linear and nonlinear biharmonic eigenvalue problems*, Stud. Appl. Math., 126 (2011), pp. 347–408.

[16] W. M. Lee and J. T. Chen, *Free vibration analysis of circular plates with multiple circular holes using indirect BIEM and addition theorem*, J. Appl. Mech., 78 (2010), 011015.

[17] A. E. Lindsay and M. J. Ward, *Asymptotics of some nonlinear eigenvalue problems modelling a MEMS capacitor. Part* II: *Multiple solutions and singular asymptotics*, European J. Appl. Math., 22 (2010), pp. 83–123.

[18] P. Laurençot and C. Walker, *A fourth-order model for MEMS with clamped boundary conditions*, arXiv:1304.2296, 2013.

[19] S. Ozawa, *Singular variation of domains and eigenvalues of the Laplacian*, Duke Math. J., 48 (1981), pp. 767–778.
[20] T. Ransford, *Potential theory in the complex plane*, London Math. Soc. Stud. Texts 28, Cambridge University Press, Cambridge, 1995.
[21] J. N. Reddy, *Theory and Analysis of Plates and Shells*, CRC Press, Boca Raton, FL, 2007.
[22] G. Sweers, *When is the first eigenfunction for the clamped plate equation of fixed sign?*, Electron. J. Differential Equations, 6 (2001), pp. 285–296.
[23] M. J. Ward, W. D. Henshaw, and J. Keller, *Summing logarithmic expansions for singularly perturbed eigenvalue problems*, SIAM J. Appl. Math., 53 (1993), pp. 799–828.
[24] M. J. Ward, and J. B. Keller, *Strong localized perturbations of eigenvalue problems*, SIAM J. Appl. Math., 53 (1993), pp. 770–798.